

Dissertation zur Erlangung des Doktorgrades
der Fakultät für Chemie und Pharmazie
der Ludwig-Maximilians-Universität München



Targeting the actin cytoskeleton with natural compounds: elucidating
the underlying mechanism of apoptosis induction

Florian Förster
aus Amberg, Deutschland
2014

Erklärung

Diese Dissertation wurde im Sinne von § 7 der Promotionsordnung vom 28. November 2011 von Frau Prof. Dr. Angelika M. Vollmar betreut.

Eidesstattliche Versicherung

Diese Dissertation wurde eigenständig und ohne unerlaubte Hilfe erarbeitet.

München, den ____ . März 2014

.....
Florian Förster

Dissertation eingereicht am:	13.03.2014
1. Gutachter:	Prof. Dr. Angelika M. Vollmar
2. Gutachter:	Prof. Dr. Stefan Zahler
Mündliche Prüfung am:	10.04.2014

MEINEM VATER

CONTENTS

Contents.....	4
1 Introduction	9
1.1 Breast cancer and current therapeutic options	10
1.2 Actin-binding compounds Chondramide A and Dolicolide	11
1.3 The actin cytoskeleton: Regulation and physiological function	12
1.4 Regulation of apoptosis.....	14
1.4.1 Extrinsic apoptosis pathway.....	14
1.4.2 Intrinsic apoptosis pathway.....	15
1.5 Mitochondrial permeability transition	16
1.5.1 Structure of the mitochondrial permeability transition pore.....	17
1.5.2 Regulation of the mitochondrial permeability transition pore	17
1.6 PKC ϵ : structure, function and implications in cancer	19
1.6.1 The structure of PKC ϵ	19
1.6.2 Activation and function of PKC ϵ	20
1.6.3 The role of PKC ϵ as oncogenic player and its role in cancer.....	21
1.7 Aim of the study	21
2 Materials and Methods.....	23
2.1 Materials	24
2.1.1 Chondramides	24
2.1.2 Dolicolide	24
2.1.3 Reagents: Biochemicals, inhibitors, cell culture reagents and technical equipment	24
2.2 Cell culture	27
2.2.1 Cell culture buffers, solutions, procedure and cell lines.....	27
2.2.2 Freezing and thawing of cells	30
2.3 Fluorescence recovery after photobleaching (FRAP)	30

2.4	Quantification of cell death	30
2.4.1	Propidium iodide exclusion assay	30
2.4.2	Analysis of membrane phosphatidylserine exposure	30
2.5	Cytochrome C release.....	31
2.6	Mitochondrial membrane potential ($\Delta\Psi_m$).....	31
2.7	Caspase 8 activity assay	31
2.8	Isolation of mitochondria from cultured cells.....	32
2.9	Western blot.....	33
2.9.1	Buffers and solutions for Western blot	33
2.9.2	Western blot, cytosolic-mitochondrial fractionation and cytosolic-cytoskeletal fractionation.....	35
2.9.3	Primary and secondary antibodies used for immunoblotting	36
2.10	Transfection of FLAG.PKC ϵ and mGFP- β -actin.....	37
2.11	Immunostaining and confocal microscopy	38
2.12	Immunohistochemistry of tissue sections	39
2.13	<i>In vivo</i> mouse xenograft model.....	39
2.14	Proliferation assay.....	40
2.15	Migration assay	40
2.16	Statistics.....	40
3	Results	41
3.1	Disrupting the actin cytoskeleton with Chondramide leads to cell death via trapping PKC ϵ	42
3.1.1	Chondramide impairs actin dynamics and leads to the induction of the intrinsic apoptotic pathway	42
3.1.2	The role of mitochondrial permeability transition in Chondramide induced cell death	48
3.1.3	Chondramide inhibits PKC ϵ by trapping it in actin bundles.....	53

3.1.4	PKC ϵ overexpression leads to cell death reduction.....	57
3.1.5	Chondramide treatment displays tumor cell specificity.....	58
3.1.6	Chondramide has anti-tumor effects <i>in vivo</i>	60
3.2	Characterization of actin-binding Dolicolide in breast cancer cells.....	63
3.2.1	Effects of Dolicolide on the actin cytoskeleton.....	63
3.2.2	Effects of Dolicolide on functional parameters of breast cancer cells.....	65
3.2.3	Dolicolide induces apoptosis.....	67
4	Discussion.....	69
4.1	Targeting the actin cytoskeleton with Chondramide A: selective anti-tumor action via trapping PKC ϵ	70
4.1.1	PKC ϵ is an interesting candidate linking the actin CSK to cell death.....	71
4.1.2	PKC ϵ is the “Bad guy” among PKCs.....	72
4.1.3	Apoptosis via MPT is modulated by PKC ϵ and affected by Chondramide.....	72
4.1.4	Chondramide is a selective indirect inhibitor of PKC ϵ	73
4.2	Pharmacological characterization of actin-binding (-)-Dolicolide.....	74
4.2.1	Dolicolide inhibits actin dynamics.....	74
4.2.2	Dolicolide inhibits functional parameters and induces apoptosis.....	74
4.3	The potential of actin targeting compounds in cancer therapy.....	75
4.4	Future perspectives.....	76
5	Summary.....	77
6	References.....	81

7	Appendix.....	86
7.1	Publications.....	87
7.1.1	Original publications	87
7.1.2	Poster presentations.....	87
7.1.3	Oral presentations	88
7.1.4	Awards	88
7.2	Curriculum vitae	Fehler! Textmarke nicht definiert.
	Personal data	Fehler! Textmarke nicht definiert.
	Academic education	Fehler! Textmarke nicht definiert.
7.3	Acknowledgements	89

1 INTRODUCTION

1.1 Breast cancer and current therapeutic options

Among women breast cancer is the most often diagnosed malignancy (1). Though a proper progress in breast cancer therapy within the last 15 years the mortality rate is still about 25 % (1). The clinical disease is described with a ranking according to the TNM (tumor, node, metastasis) staging system, which can be divided in four stagings (with subdivisions) (2). Furthermore, the histological and genetic characterization is also important for the classification of mamma carcinomas. E.g. the status of estrogen- and progesterone receptor is determined via histological stainings and the status of the BRCA1 and BRCA2 (Breast Cancer, early onset 1 and 2) gene can be determined via a genetic analysis giving implications for clinical treatment and prognosis (3). According to the respective staging of the tumor the therapy is adjusted. In sum, there are three general therapeutic options how breast cancer can be treated: The first is surgery and if possible complete excision of the tumor tissue, second, radiation of the tumor or tumor surrounding tissue and third pharmacological intervention (4). Pharmacological therapy can be further subdivided in hormone therapy, targeted therapy and classical chemotherapy. Hormone therapy can be used for tumors expressing estrogen receptors. Commonly used drugs are aromatase inhibitors like Anastrozol or selective estrogen-receptor modulators like Tamoxifen (5). The group of targeted therapy contains drugs like Trastuzumab, an antibody directed against the growth factor receptor HER2/neu, or Lapatinib, a receptor-tyrosine-kinase inhibitor (Erb1 and HER2/neu) (6). The largest group of drugs against mamma carcinomas are classical chemotherapeutics. Different classes of chemotherapeutics are used against breast cancer: For instance, alkylants like Cisplatin and Cyclophosphamide, antimetabolites like Methotrexate and Fluoruracil, anthracyclins like Doxorubicin and taxanes like Paclitaxel or Docetaxel (1). All of the above mentioned chemotherapeutics show partially strong adverse effects that can be dose-limiting or even lead to the abrogation of chemotherapy. E.g. Doxorubicin is known to be cardiotoxic in a dose-cumulative manner, whereas taxanes are strongly related to neurotoxicity (7, 8). Furthermore, a broad variety of resistance mechanisms against almost every chemotherapeutic agent is known, which further limits the efficacy of today's anti-cancer drugs (9). Thus, research for new targets and compounds is still necessary to strengthen the phalanx of anti-cancer drugs against human malignancies.

1.2 Actin-binding compounds Chondramide A and Dolicolide

One emerging source of potential new anti-cancer drugs are the myxobacteria. Approximately 7500 identified myxobacterial strains have yielded at least 100 distinct core structures (10). Among them are also the Chondramides. Another source for natural derived compounds are marine organisms. They also possess a broad biodiversity containing organisms producing potential anti-cancer structures in their secondary metabolism (11). Chondramide A (**Fig. 1.1 A**) was first isolated from *Chondromyces crocatus* in 1995 and showed cytostatic properties on mammalian cell lines (12). Dolicolide (**Fig. 1.1 B**) was first extracted from *Dolabella auricularia* a sea hare in 1994 and is cytotoxic towards HeLa cells, a cervix carcinoma cell line (13, 14). Both compounds share common structural features as they are both cyclodepsipeptides. Chondramide A consists of 18 atoms in the ring whereas Dolicolide has 16 atoms (14, 15). Regarding their similar structure it is not surprising that Chondramide A and Dolicolide also share the same target structure. It was shown for both compounds that they compete with Phalloidin, known to bind to filamentous actin, to the actin binding site (16). The Phalloidin-binding site on actin, probably also the binding-site of Chondramide A and Dolicolide, was characterized by microscopic and X-ray diffraction methods and appears to interact with three actin monomers simultaneously (17-19). The binding of the three compounds to actin lead to the stabilization and overpolymerization of the actin cytoskeleton. The contrary effect a de-stabilization is also known for other natural compounds binding to actin e.g. Rhizopodin or Cytochalasin D (16). Though those compounds are strong inhibitors of mammalian cancer cell growth none of those compounds has ever been brought to clinical trials. The reasons for it might range from poor membrane permeability for Phalloidin to cardiotoxic effects for Jasplakinolide to the fact that no closer mechanistic insight how cell death might be established through the disruption of the actin cytoskeleton has ever been gained (20-22). Thus, Chondramide A and Dolicolide were used as tools to examine the potential of actin as anti-cancer target.

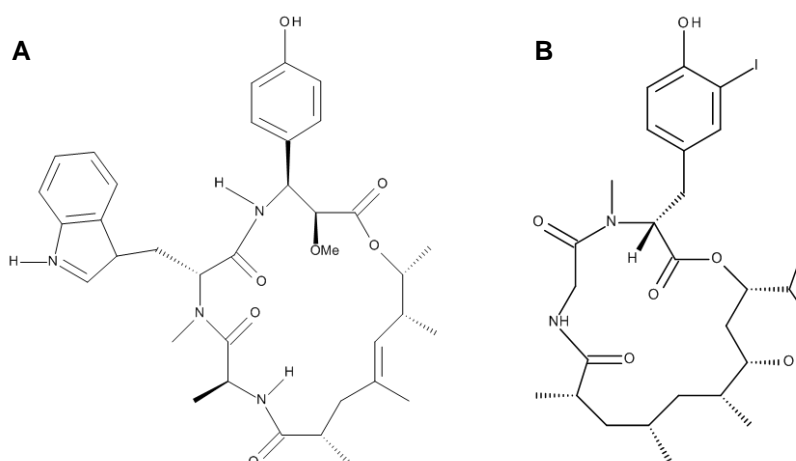


Figure 1.1: Chemical structures of (A) Chondramide A and (B) (-)-Doliculide.

1.3 The actin cytoskeleton: Regulation and physiological function

Next to microtubules and the intermediate filaments, actin filaments also called microfilaments form the third column of the cellular cytoskeleton (CSK) of eukaryotes (23). Monomeric actin proteins exist in six isoforms (α_1 , α_2 , α_{cardiac} , β , γ_1 and γ_2) and show a tissue specific distribution (24). Monomeric or globular actin (g-actin) is able to polymerize to polarized, helical actin filaments (f-actin) in an ATP dependent manner. Globular actin monomers nucleate at a minimal concentration of four monomers and elongate faster on the barbed end whereas they slowly depolymerize on the pointed end (23). The polymerization of actin is a dynamic process in which the ATP-bound to actin gets hydrolyzed to ADP and P_i and leads to the severing of the actin monomer from the filament. The free globular actin monomer can be recharged with ATP and again be implemented in the growing actin filament. This circle of globular and filamentous actin is also called treadmilling (**Fig. 1.2 A**) (25). A variety of more than 100 proteins participate in the regulation of actin dynamics (23). The most famous actin-binding proteins controlling actin dynamics are for example: severing proteins like Cofilin/ADF and Gelsolin, branching proteins like the Arp2/3 complex or proteins promoting nucleation and elongation like the Formins and WASP (**Fig. 1.2 B**) (23, 26). This complex regulation of the actin CSK primes it for important functions in an eukaryotic cell. The actin CSK is very important for the form and structure of the cell and for its adhesion to other cells or the basal lamina (27). Furthermore, actin plays a crucial role during cytokinesis, via forming the contractile ring, during endocytosis, by delivering the force for clathrin-mediated vesicle transport, and

migration of motile cells, by pulling forward the cell body (23). Changes in actin dynamics are also known to interfere with the induction of apoptosis. Pharmacological perturbations of the actin CSK with overpolymerizing compounds like Jasplakinolide or depolymerizing compounds like Cytochalasin D are known to lead to apoptosis, but closer mechanistic insights are still elusive (22).

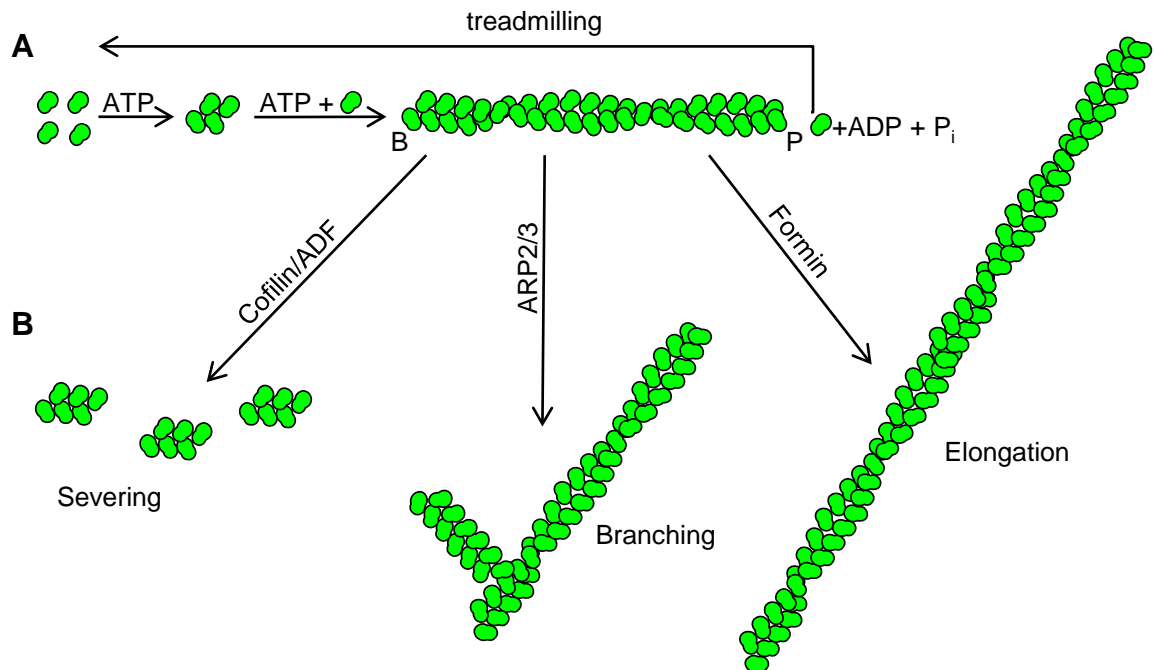


Figure 1.2: Regulation of actin dynamics. (A) Four actin monomers are necessary to form a nucleus from which polymerization can start. Polymerization is faster on the barbed end (B), whereas on the pointed end (P) ATP gets hydrolyzed and an actin monomer is severed from the filament. The monomer can be recharged with ATP and can be reused for polymerization on the barbed end. This process is called treadmilling. (B) Actin-binding proteins and their different functions in regulation of filament structure. Cofilin/ADF severs filaments into globular actin monomers, ARP2/3 is a typical branching protein and Formin promotes elongation of actin filaments.

1.4 Regulation of apoptosis

Apoptosis or programmed cell death was first described in 1972 by Kerr et al. (28) and was characterized as a new type of cell death different from necrosis. Meanwhile it is known that apoptosis is a major factor for tissue homeostasis and it is a well-known fact that cancer cells possess various ways to evade apoptosis and gain unlimited proliferative capacities to establish their deleterious network (29-31). Some morphological and cellular hallmarks of apoptosis are the blebbing of the plasma membrane, nuclear condensation and fragmentation, and the transition of phosphatidyl serine from the inner leaflet of the plasma membrane to the outer leaflet (32). The main class of proteins that are responsible for the morphological and cellular changes of apoptotic cells are the caspases. Caspases (cysteiny-l-aspartate specific proteases) are a family of cysteine proteases which contain cysteine residues at their active site and cleave their substrate at a position next to an aspartate residue (33). Caspases can be grouped into initiator- and effector caspases and depending on the mechanism how specific initiator caspases are activated at least two different apoptosis pathways can be distinguished (32). These two different induction mechanism will be highlighted in the following chapter.

1.4.1 Extrinsic apoptosis pathway

The extrinsic apoptotic pathway is induced by a ligand (e.g. Tumor necrosis factor α (TNF α) or Tumor necrosis factor related apoptosis inducing ligand (TRAIL)) binding to its so-called death-receptor (e.g. TRAIL-receptors 1 and 2) (29). Once the ligand binds to its receptor the cascade that starts is very similar between the different ligand/receptor complexes. The activation of the death receptors causes the recruitment and oligomerization of the adapter protein FADD (Fas-associating death domain-containing protein) within the death-inducing signaling complex (DISC). DISC cleaves the initiator Caspase 8 in its active form which further activates downstream effector Caspases 3 and 7 (32). There is a crosslink between the extrinsic and intrinsic apoptotic pathway via the BH3-only protein Bid that is truncated by Caspase 8 and leads to mitochondrial membrane permeabilization (34). Mitochondrial membrane permeabilization is also the crucial hallmark of the intrinsic apoptotic pathway (**Fig. 1.3 A**).

1.4.2 Intrinsic apoptosis pathway

The stimuli for intrinsic apoptotic cell death are multifactorial and range from DNA-damage over oxidative and ER stress to metabolic disorders (32, 35). Independent of the origin of the death signal the crucial step of the intrinsic pathway is the release of proteins from the intermembrane space of mitochondria to the cytosol. One major protein that is released is Cytochrome C. Once in the cytosol Cytochrome C forms a multi protein complex with APAF1 and Caspase 9, the so called Apoptosome. This leads to the activation of the initiator Caspase 9 and the subsequent activation of the effector Caspases 3, 6 and 7 and the induction of subsequent cellular demolition (**Fig. 1.3 B**) (29, 36).

Crucial regulators and mediators of stress signals to the mitochondria are the proteins belonging to the Bcl-2 family (32). The name derives from the role model molecule that is genetically altered in B-cell lymphoma. These proteins are characterized by the presence of at least one Bcl-2 homology (BH) domain. Bcl-2 proteins can be divided in two groups: the anti-apoptotic Bcl-2 proteins consisting of e.g Bcl-2, Bcl-X_L and Mcl-1 and the pro-apoptotic Bcl-2 proteins containing the proteins e.g Bax, Bak, Bad, Bid, Noxa and PUMA. All these proteins are regulated via transcriptional, post-translational and protein-protein interactions among the members of this class (37).

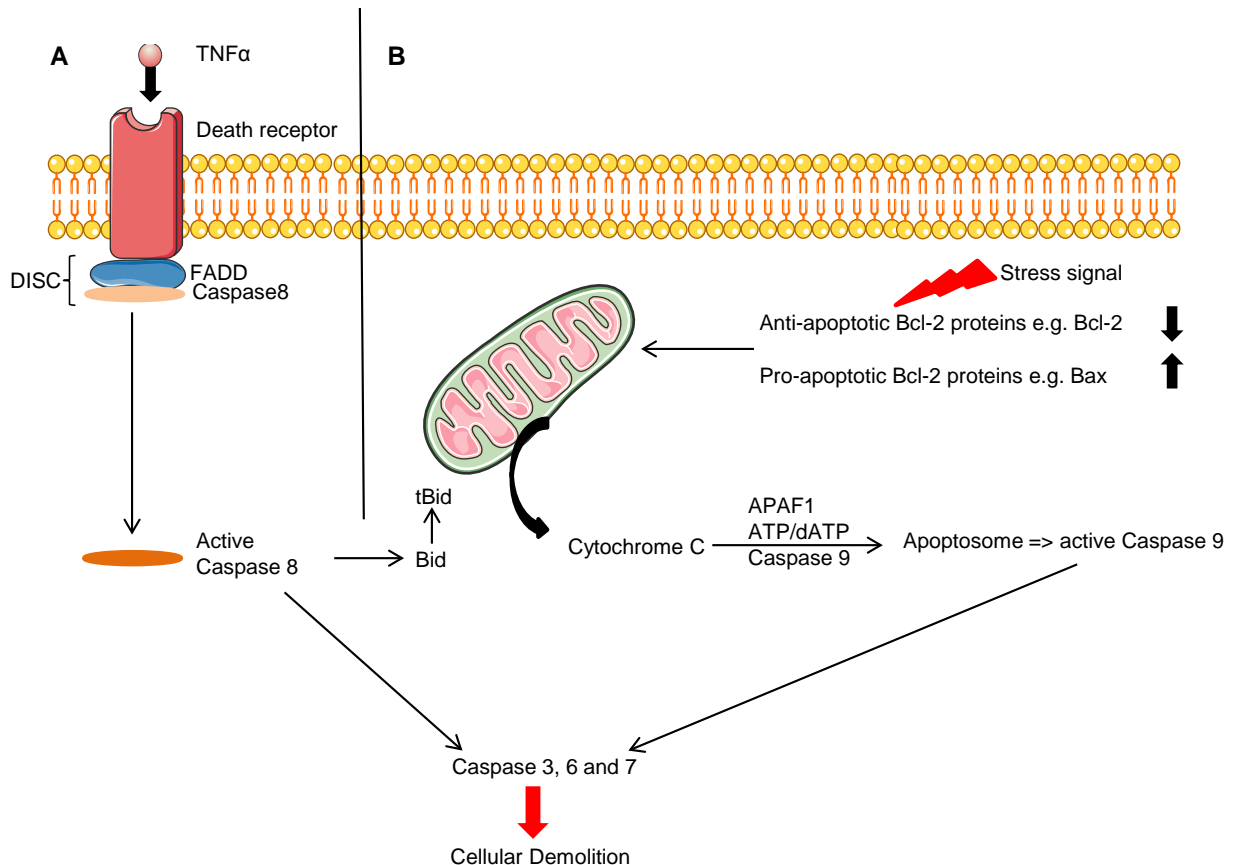


Figure 1.3: Mechanisms of apoptosis induction: (A) Extrinsic pathway: A ligand like TNF α binds to its receptor (death receptor) and activates the formation of the death-inducing-signaling-complex (DISC) consisting of FADD and Caspase 8, leading to Caspase 8 activation. Active Caspase 8 cleaves the effector caspases 3, 6 and 7 into active forms and can also co-activate the intrinsic apoptotic pathway by cleaving Bid into truncated Bid (tBid), which leads to Cytochrome C release from mitochondria. (B) Several stress signal lead to a change of the ratio between anti- and pro-apoptotic Bcl-2 proteins, switching it on the site of the pro-apoptotic ones (like Bax). This leads to the permeabilization of mitochondria and the release of Cytochrome C. Cytochrome C, APAF1, ATP/dATP and Caspase 9 form the active Apoptosome and active Caspase 9 leads to the activation of the effector caspases 3,6 and 7, which results in cellular demolition.

1.5 Mitochondrial permeability transition

Main hallmark of the intrinsic apoptotic pathway is mitochondrial membrane permeabilization. Next to mitochondrial outer membrane permeabilization (MOMP), mitochondrial permeability transition (MPT) via the mitochondrial permeability transition pore complex is the major pathway how intermembrane space proteins can be released from mitochondria (29). The exact composition of the pore complex is controversial, but a consensus model established within the last decade which will be promoted in this chapter (29, 38).

1.5.1 Structure of the mitochondrial permeability transition pore

The mitochondrial permeability transition pore (MPTP) is a multi-protein complex located on the contact sites of inner mitochondrial membrane (IMM) and outer mitochondrial membrane (OMM) (38). It consists of Cyclophilin D in the inner lumen of mitochondria, the adenosine-nucleotide-transporter (ANT) in the IMM, the voltage-dependent-anion-channel (VDAC) in the OMM and Hexokinase II (HkII) located on the cytoplasmic site (**Fig. 1.4**). Other proteins like the peripheral benzodiazepine receptor (PBR) or creatinin-kinase (CK) are also discussed to be part of the MPTP (38). The MPTP is supposed to fulfill functions in maintaining mitochondrial homeostasis, by transporting H₂O, ions and solutes < 1500 Dalton, and induction of cell death (38). Upon a sustained opening of MPTP a release of Cytochrome C from the inter-membrane space (IMS) can be observed. How exactly Cytochrome C is released is still a matter of debate. The way directly through MPTP is unlikely. It is more plausible that solutes enter the mitochondria via the open MPTP, thus leading to the swelling of mitochondria and finally to the disruption of the OMM and the respective release of IMS proteins (39, 40). The release of IMS proteins then results in the induction of apoptosis.

1.5.2 Regulation of the mitochondrial permeability transition pore

In the context of this work especially the regulation of the MPTP is crucial. Several proteins of the putative multi-protein complex are known to regulate the opening probability of the pore. The only verified protein of the pore is Cyclophilin D located in the inner lumen of mitochondria. Upon opening of the pore Cyclophilin D locates to the multi-protein complex and facilitates in the release of IMS proteins (41). The participation of Cyclophilin D can pharmacologically be inhibited via Cyclosporine A that prevents the binding of Cyclophilin D to the other pore proteins (42). This property is often used in assays working with isolated mitochondria to detect a participation of MPTP (43). Another protein interaction is also known to regulate the opening of the pore, namely the interaction between VDAC in the OMM and HkII on the cytoplasmic site. When HkII is associated to VDAC the MPTP is in a closed conformation (44). Whereas, when HkII dissociates from VDAC the opening probability of MPTP is increased. Another regulation of the pore is achieved via proteins belonging to the Bcl-2 family. The BH-3 only protein Bad is described to be able to open the MPTP, when Bad is dephosphorylated on Serine residue 112 resulting in its activation (45). This is supposed to happen via an interaction with Bcl-X_L, an anti-apoptotic member of the Bcl-2 family that is physiologically located in the OMM and facilitates the closure of MPTP. Active Bad interacts with Bcl-X_L and prevents it from closing the MPTP (**Fig. 1.4**) (45). The interaction of HkII/VDAC and

Bad/Bcl-X_L are known to be regulated by a serine-/threonine kinase from the PKC family named PKC ϵ .

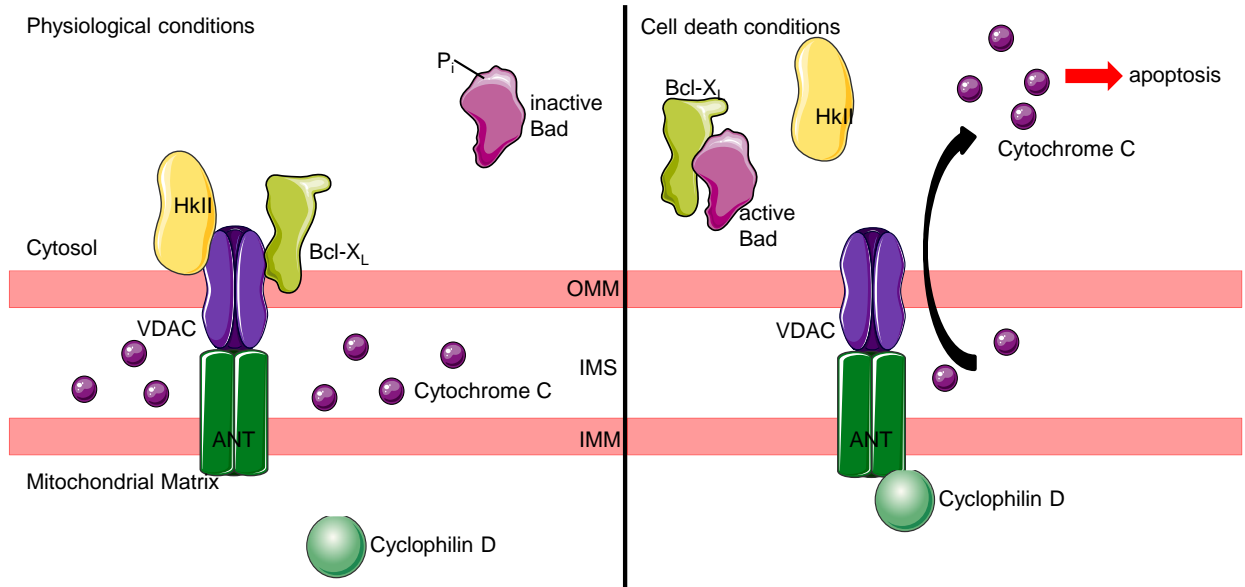


Figure 1.4: Structure and regulation of the mitochondrial permeability transition pore: Physiological conditions: Bad is phosphorylated, inactive and rests in the cytosol. Hexokinase II (HkII) and Bcl-X_L stabilize the MPTP and prevent its opening. The voltage-dependent-anion-channel (VDAC) is located in the outer mitochondrial membrane (OMM) and the adenosine-nucleotide-translocase (ANT) in the inner mitochondrial membrane (IMM). Cyclophilin D is located in the mitochondrial matrix. Cell death conditions: Cyclophilin is recruited to ANT and facilitates opening of MPTP, HkII translocates from VDAC to the cytosol preferring the opening of MPTP and dephosphorylated, active Bad interacts with Bcl-X_L also enabling the opening of MPTP. This results in a release of Cytochrome C from the intermembrane space (IMS) to the cytosol resulting in apoptosis.

1.6 PKC ϵ : structure, function and implications in cancer

The protein kinase C family (PKC) consists of eleven members, that regulate a wide variety of cellular functions (46). The PKC family is further subdivided into three classes named the classical PKCs ($\alpha, \beta I, \beta II$ and γ), the novel PKCs (δ, θ, ϵ and η) and the atypical PKCs ($\zeta, \iota/\lambda$) (47). The classes differ in the way they are activated. In our context one PKC is of special interest: PKC ϵ .

1.6.1 The structure of PKC ϵ

The overall structure of PKC ϵ is very similar to other PKCs. It consists of a regulatory domain containing the C2-like region responsible for binding phospholipids and membrane localization of active PKC ϵ , a pseudo-substrate region and the C1 domain that is splitted into the C1A and C1B region (Diacylglycerol and phorbol 12-myristate 13-acetat bind to the C1 domain). A hinge region connects the regulatory domain and the kinase domain consisting of the C3 and C4 region. Within the C1 domain a structural feature, an actin-binding-site is contained, that is unique to PKC ϵ (**Fig. 1.5**) (47-49).

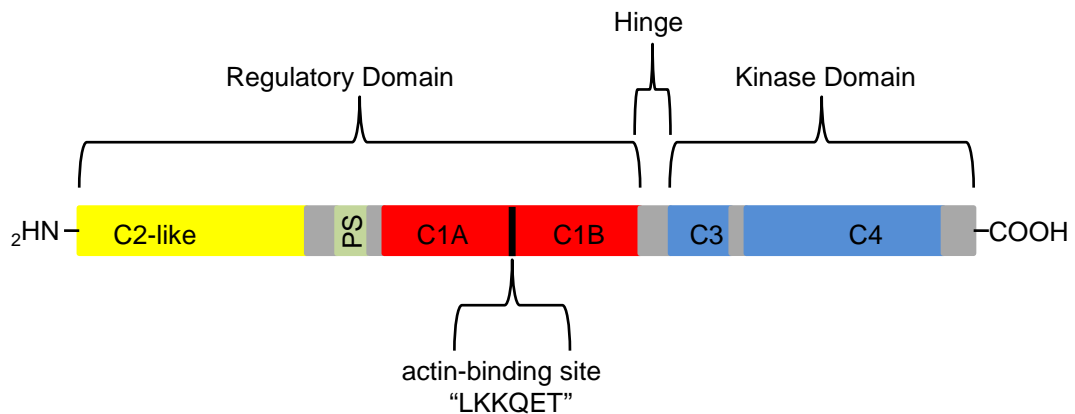


Figure 1.5: Structure of PKC ϵ .

1.6.2 Activation and function of PKC ϵ

Agonist stimulation of several g-protein-coupled receptors and tyrosine kinase receptors can activate Phospholipase C (PLC). PLC facilitates the production of Diacylglycerol (DAG), hence the activation of PKC ϵ (48). Other activators of PKC ϵ are fatty acids like arachidonic acid or phorbol 12-myristate 13-acetate (PMA) (47). Upon activation PKC ϵ is either localized to the cell membrane where DAG is bound or to so called RACKS (receptor of activated protein C kinases) that are located at intracellular membranes like the Golgi. Binding to the membrane leads to conformational changes of PKC ϵ and substrate binding in the kinase domain can take place (50). Once activated PKC ϵ has a broad variety of downstream targets. Among others PKC ϵ regulates STAT3 activity by Ser727 phosphorylation (51), activates NF- κ B (52) or increases protein levels of anti-apoptotic Bcl-2 (53). Furthermore, PKC ϵ is also known to regulate the opening probability of MPTP: One parameter regulated by PKC ϵ is the interaction between VDAC and HkII. Several mechanisms seem to be plausible: First, VDAC could be directly phosphorylated by PKC ϵ strengthening the interaction between VDAC and HkII (54). Second, the interaction between VDAC and HkII might be indirectly regulated by PKC ϵ via the transcription factor ATF2 (55). Another MPTP regulator controlled by PKC ϵ is the pro-apoptotic BH3-only protein Bad. PKC ϵ can directly phosphorylate Bad on Ser112 and keep Bad in its inactive conformation (56).

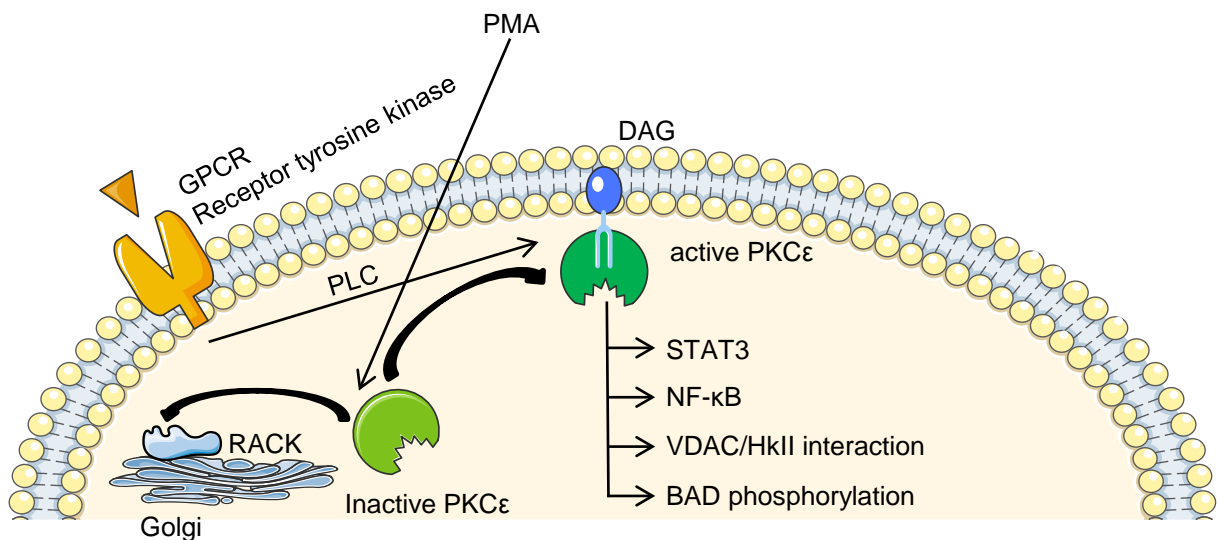


Figure 1.6: PKC ϵ activation and downstream targets: Upon agonist stimulation of GPCRs or receptor tyrosine kinases Phospholipase (PLC) generates membrane-anchored Diacylglycerol (DAG), which activates PKC ϵ . PKC ϵ can also artificially be activated via exogenous PMA. Upon activation PKC ϵ either translocates to the cell membrane or to intracellular receptors of activated protein C kinase (RACK) located on intracellular compartments like the golgi. PKC ϵ regulates among others the transcription factors STAT3 and NF- κ B and exerts pro-survival signals via stabilizing the VDAC/HkII interaction and the phosphorylation of BAD on Ser112, thus preventing the opening of MPTP.

1.6.3 The role of PKC ϵ as oncogenic player and its role in cancer

The regulation of NF- κ B and Stat3 already indicates a pro-survival and oncogenic function of PKC ϵ . Also other oncogenic functions for PKC ϵ were described: PKC ϵ was shown to increase tumorigenicity of non-cancer cells, increases metastatic potential and resistance to chemotherapy and irradiation (57-59). Furthermore, PKC ϵ is also known to be overexpressed in certain human malignancies and linked to poor prognosis e.g. in breast cancer and gliomas (60, 61). PKC ϵ is the only PKC isoform considered to have a massive oncogenic potential (50). This primes PKC ϵ as a promising anti-tumor target, but approaches to target PKC ϵ selectively failed so far, because inhibition with small molecules lack isoform specificity (62).

Because of its role as oncogene, its actin-binding site and its implications in controlling the MPTP, PKC ϵ is an interesting candidate linking the disruption of the actin CSK by Chondramide to cell death.

1.7 Aim of the study

Evading apoptosis is a major hallmark of cancer cells. Commonly used chemotherapies aim to drive cancer cells into apoptosis and to stop tumor growth. Though the ubiquitous microtubule network is a cancer target for decades, another important cytoskeletal network the actin cytoskeleton is not targeted by any clinically used drug so far. Thus, we used the actin-binding compounds Chondramide A and Dolicolide to describe their potential to stimulate apoptotic cell death in breast cancer cells. Furthermore, we wanted to explore the cell death inducing mechanism that is behind the disruption of the actin cytoskeleton and use Chondramide A for this purpose. An interesting signaling player connecting the actin cytoskeleton and cell death is PKC ϵ with its actin-binding site. PKC ϵ might be the key player to link intrinsic apoptosis via the mitochondrial permeability transition pore complex to cell death induction by Chondramide A. Furthermore, we have also been interested in the question whether there is any selectivity between cancerous and non-cancerous cells towards Chondramide A induced toxicity and the link to PKC ϵ expression level (**Fig. 1.7 A**).

Besides, we want to characterize another actin-binding compound namely Dolicolide on its effects: first on the actin cytoskeleton, second functional characteristics of cancer cells like proliferation and migration and third on its impact on apoptosis induction (**Fig. 1.7 B**).

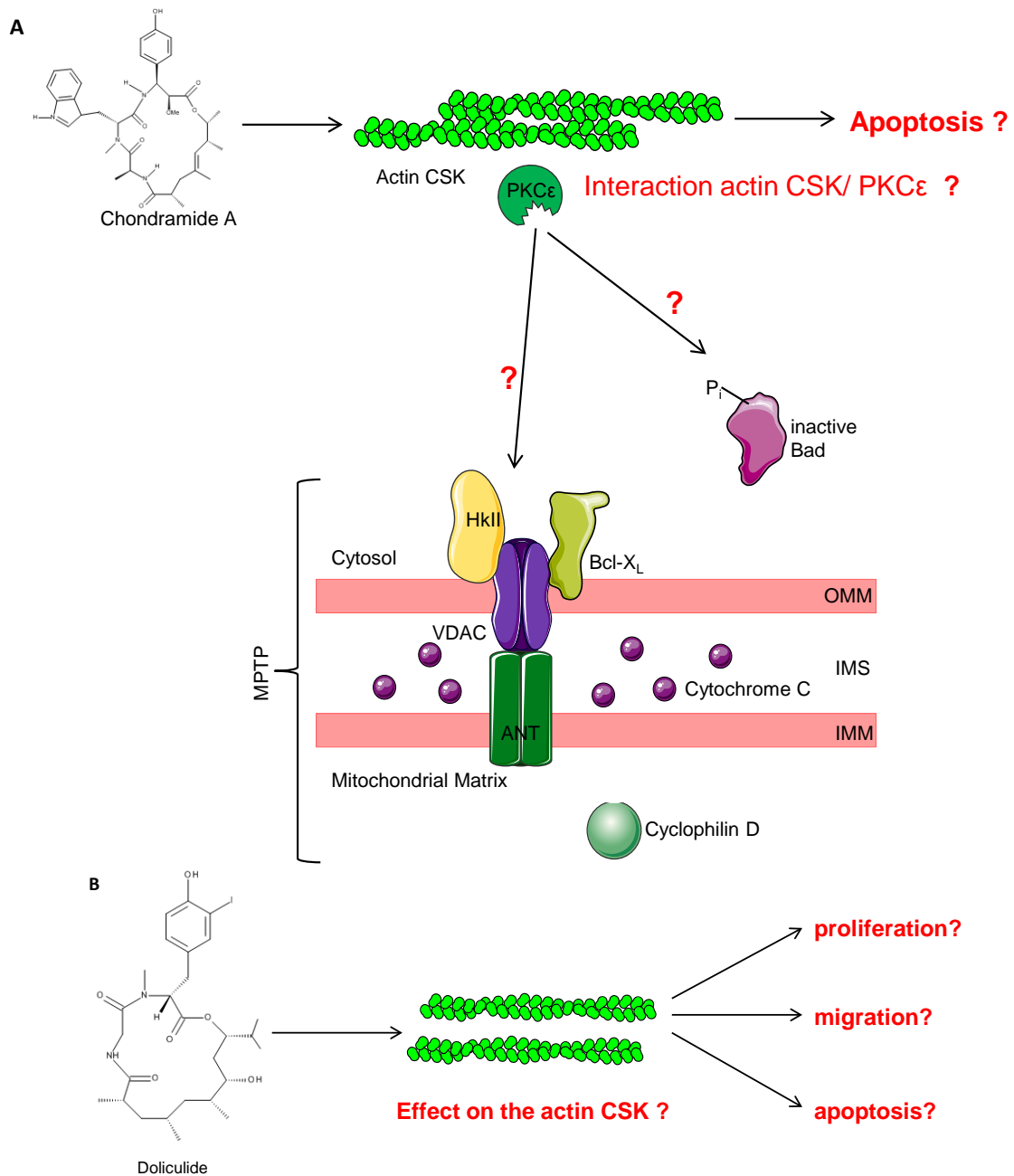


Figure 1.7: (A) One aim of the study is to investigate the effects of Chondramide A treatment on the actin cytoskeleton (Actin CSK) and the subsequent downstream signaling leading to apoptosis. Of special interest in this context is PKC ϵ as it contains an actin-binding site and might be affected by Chondramide A treatment. Downstream of PKC ϵ we are interested in proteins regulating the mitochondrial permeability transition pore (MPTP), namely VDAC/HklII interaction and Bad phosphorylation. **(B)** The second aim of the study was to investigate the effects of Dolicolide on the actin CSK and basic functional parameters like proliferation, migration and apoptosis induction.

2 MATERIALS AND METHODS

2.1 Materials

2.1.1 Chondramides

Myxobacterial cyclodepsipeptides Chondramide A and B were provided by the group of Rolf Müller (Department of Pharmaceutical Biotechnology, Saarbrücken, Germany). Chondramide A was used in *in vitro* cell culture experiments, whereas Chondramide B was used in animal experiments, because of its higher abundance. Chondramide A was dissolved in DMSO at a concentration of 1 mM and aliquots were stored at – 20° C. For stimulation a 10 x overconcentrated solution in medium was prepared and added in concentrations as indicated in figures.

2.1.2 Dolicolide

(-)-Doliculide was synthesized by the group of Karlheinz Altmann (Pharmaceutical Biology, ETH Zürich, Switzerland) and dissolved in DMSO at a concentration of 1 mM. Aliquots were stored at – 20° C. For stimulation the same procedure as for Chondramide A was performed.

2.1.3 Reagents: Biochemicals, inhibitors, cell culture reagents and technical equipment

Biochemicals

Reagent	Producer
Amaxa Nucleofector Kit V	Lonza, Köln, Germany
Annexin-V-FITC Apoptosis detection Kit	ebioscience, Vienna, Austria
β-mercaptoethanol	Merck, Darmstadt, Germany
Bovine Serum Albumine (BSA)	Sigma-Aldrich, Taufkirchen, Germany
Bradford reagent Roti® Quant	Carl Roth, Karlsruhe, Germany
CellTiterBlue reagent	Promega, Mannheim, Germany
Digitonin	Sigma-Aldrich, Taufkirchen, Germany
Dimethylsulfoxide (DMSO)	Sigma-Aldrich, Taufkirchen, Germany
ECL Plus WB Detection reagent	GE Healthcare, München, Germany
FluorSave® reagent mounting medium	Merck, Darmstadt, Germany

Formaldehyde-Solution 10% PBS buffered	Applichem, Darmstadt, Germany
FuGENE® HD transfection reagent	Promega, Mannheim, Germany
Glutamine	Sigma-Aldrich, Taufkirchen, Germany
Glycerol	Applichem, Darmstadt, Germany
HEPES	Carl Roth, Karlsruhe, Germany
JC-1 iodide	Axxora, Lörrach, Germany
Mannitol	Merck, Darmstadt, Germany
Mitotracker Red CMXRos	Invitrogen, Karlsruhe, Germany
Na ₂ EGTA	Applichem, Darmstadt, Germany
Na ₂ EDTA	Carl Roth, Karlsruhe, Germany
Non-fat dry milk powder	Carl Roth, Karlsruhe, Germany
PAGE Ruler® Prestained Protein Leader	Fermentas, St. Leon-Rot, Germany
Phorbol-13-myristate-12-acetate (PMA)	Merck Millipore, Billerica, MA, USA
Polyacrylamide	Carl Roth, Karlsruhe, Germany
Propidium iodide	Sigma-Aldrich, Taufkirchen, Germany
Pyronine Y	Applichem, Darmstadt, Germany
Rhodamin 123	Sigma-Aldrich, Taufkirchen, Germany
Rhodamin-Phalloidin	Invitrogen, Karlsruhe, Germany
Saccharose	Carl Roth, Karlsruhe, Germany
Sodium chloride	Carl Roth, Karlsruhe, Germany
Sodiumdodecylsulfate (SDS)	Carl Roth, Karlsruhe, Germany
Sodiumglycerolphosphate	Applichem, Darmstadt, Germany
Tris Base	Sigma-Aldrich, Taufkirchen, Germany
Triton X-100	Merck, Darmstadt, Germany
Tunel ApopTag® apoptosis detection Kit	Merck Millipore, Billerica, MA, USA

All other biochemical reagents were purchased by Carl Roth, Sigma-Aldrich or Merck.

Inhibitors

Inhibitor	Producer
Ciclosporine A	Sigma-Aldrich, Taufkirchen, Germany
Complete® mini EDTA free	Roche diagnostics, Penzberg, Germany
NaF	Merck, Darmstadt, Germany
Na ₃ VO ₄	ICN, Biomedicals, Aurora, OH, USA
Phenylmethylsulfonyl fluoride (PMSF)	Sigma-Aldrich, Taufkirchen, Germany

Cell culture reagents

Cell culture reagent	Producer
Cholera Toxin	Sigma-Aldrich, Taufkirchen, Germany
Collagene G	Biochrom AG, Berlin, Germany
DMEM/High glucose	PAA Laboratories, Pasching, Austria
EGF	Peprtech, Rocky Hill, NJ, USA
Fetal calf serum (FCS)	PAN Biotech, Aidenbach, Germany
Horse serum	Invitrogen, Karlsruhe, Germany
Hydrocortison	Sigma-Aldrich, Taufkirchen, Germany
Insulin	Sigma-Aldrich, Taufkirchen, Germany
Non-essential amino acids (NEAA)	PAA Laboratories, Pasching, Austria
Penicillin/Streptomycin 100x	PAA Laboratories, Pasching, Austria
Pyruvate	Merck, Darmstadt, Germany
RPMI 1640	PAA Laboratories, Pasching, Austria
Trypsin	PAN Biotech, Aidenbach, Germany

Technical Equipment

Name	Device	Producer
ABI 7300	RT-PCR System	Applied Biosystems, Fosterer City, CA, USA
Axiovert 200	Invert microscope	Zeiss, Jena, Germany

Culture flasks, plates and dishes	Disposable cell culture material	TPP, Trasadingen, Switzerland
Curix 60	Tabletop film developer	Agfa, Köln, Germany
FACSCalibur	Flow cytometer	Becton Dickinson, Heidelberg, Germany
Ibidi® μ -slide	Microscope slide	Ibidi GmbH, Martinsried, Germany
LSM 510 Meta	Confocal laser scanning microscope	Zeiss, Jena, Germany
Micro 22 R	Table centrifuge	Hettich, Tuttlingen, Germany
Nanodrop RND 1000	Spectrophotometer	Peqlab, Wilmington, DE, USA
Odyssey 2.1	Infrared imaging system	Li-Cor Biosciences, Lincoln, NE, USA
SpectraFluor®PLUS	Microplate multifunctional reader	Tecan, Männedorf, Switzerland
Sunrise®	Microplate absorbance reader	Tecan, Männedorf, Switzerland
Vi-Cell® CR	Cell viability and counting system	Beckmann Coulter, Fullerton, CA, USA

2.2 Cell culture

2.2.1 Cell culture buffers, solutions, procedure and cell lines

Following buffers and solutions were used for cultivation of breast cancer cell lines.

Commonly used buffers and solutions

PBS (pH 7,4)		PBS + Ca²⁺/Mg²⁺ (pH 7,4)	
NaCl	123,2 mM	NaCl	137 mM
Na ₂ HPO ₄	10,4 mM	KCl	2,68 mM
KH ₂ PO ₄	3,2 mM	Na ₂ HPO ₄	8,10 mM
H ₂ O		KH ₂ PO ₄	1,47 mM
		MgCl ₂	0,25 mM
		CaCl ₂	0,7 mM
		H ₂ O	
Trypsin/EDTA		Collagen G	
Trypsin	0,05 %	Collagen G	0,001 %
EDTA	0,20 %	PBS	
PBS			

The human epithelial breast cancer cell line MCF7 was purchased from the DSMZ (Braunschweig, Deutschland) and maintained in RPMI 1640 medium supplemented with 10 % heat inactivated fetal calf serum, 1% pyruvate, 125µg/l insulin, 1% non-essential amino acids and 1% penicillin/streptomycin. The mammary gland adenocarcinoma cell line MDA-MB-231 was purchased from cell lines service (Eppelheim, Germany) and maintained in DMEM high glucose supplemented with 10% FCS and 1% penicillin/streptomycin. MCF10-A non-tumorigenic epithelial cells were from ATCC (Manassas, VA, USA) and cultivated in RPMI 1640 medium supplemented with 5% horse serum, Insulin 125µg/l, EGF 100ng/ml, Hydrocortison 0,8µg/ml, Cholera-Toxin 0,16µg/ml and 1% penicillin/streptomycin. All cell lines were maintained in a humidified incubator at 37°C and 5 % CO₂. For passaging cells culture medium was discarded and the cell layer was washed with PBS and incubated with 3 ml Trypsin/EDTA (T/E) for several minutes at 37°C until all cells detached. T/E was stopped by adding 7 ml of the respective medium (containing 10 % FCS), cells were counted with the Vi-Cell system, centrifuged (1000 rpm, 5 minutes), resuspended and either passaged or seeded in culture dishes. MCF-7 and MDA-MB-231 were splitted in a 1:10 ratio, whereas MCF-10A cells were passaged in a

ratio of 1:5. As cell density is of enormous impact on the result of an experiment, especially with a high abundance target like actin, the cell density was kept equal to about 30000 cells/cm² if possible. Additionally, flasks and dishes for MCF-7 were coated with Collagen G solution for 5 minutes, before the MCF-7 cells were seeded.

2.2.2 Freezing and thawing of cells

For freezing cells were trypsinized, resuspended in culture medium and counted. 2×10^6 cells in 1 ml freezing medium (containing 20 % FCS + 10 % DMSO) were frozen in cryovials first at -20°C overnight, then at -80°C and few days later the cryovials were stored in nitrogen tanks (-196°C) for long-term storage.

For thawing cells were warmed up in a water bath at 37°C , then they were resuspended in culture medium and excessive DMSO was separated by centrifugation. The cell pellet was resuspended in culture medium and grown in a 25 cm² flask.

2.3 Fluorescence recovery after photobleaching (FRAP)

To analyze rapid changes in actin dynamics FRAP assay was performed. MCF7 cells transfected with mGFP- β -actin were seeded in ibidi[®]- μ -slides and incubated in the climate chamber of a Zeiss LSM 510 confocal microscope at 5% CO₂, 37°C and humidified atmosphere. Regions of interest (ROI) of equal size were chosen in untreated and Chondramide (300nM, 0.5 h) treated cells and were bleached by high laser energy (488 nm). Images were taken every five seconds lasting for approximately 2,5 minutes and the fluorescence intensity within the ROI was measured. Cells were randomly chosen for bleaching and quantification of fluorescence recovery was done using the LSM image browser software (Zeiss, Jena, Germany).

2.4 Quantification of cell death

2.4.1 Propidium iodide exclusion assay

Cells were harvested on ice, washed, exposed to a solution of propidium iodide (5 $\mu\text{g}/\text{ml}$) in PBS and immediately analyzed by flow cytometry using a Becton Dickinson FACSCalibur. Cells permeable for Propidium iodide were considered as dead. Data were analyzed by using FlowJo 7.6 software.

2.4.2 Analysis of membrane phosphatidylserine exposure

Phosphatidylserine switch to the outer leaflet of the plasma membrane was analyzed by Annexin-V staining using the respective apoptosis detection kit according to manufacturer's instructions. Cells were analyzed by a FACSCalibur cytometer. Cells

positive for Annexin-V-FITC were considered to be early apoptotic, cells positive for Annexin-V-FITC and Propidium iodide were considered to be late apoptotic and cells positive for Propidium iodide only were considered to be necrotic. Data analysis was performed using FlowJo 7.6 software.

2.5 Cytochrome C release

To detect Cytochrome C release from mitochondria, residual Cytochrome C in mitochondria was measured via flow cytometry. Cells were harvested and incubated in a digitonin-containing buffer for 30 min on ice (0.2mM Na-EGTA, 100mM KCl, 50µg/ml digitonin, PBS), fixed with 4% PFA for 20 min and unspecific binding was blocked (3% BSA, 0.05% Saponine, 1h, RT) before incubation with Cytochrome C antibody over night at 4°C and staining with the secondary antibody for 1h. Cytochrome C antibody was purchased from Cell Signaling Technology (Danvers, MA, USA) and secondary goat-anti-rabbit-Alexa-488 antibody was obtained from Invitrogen (Darmstadt, Germany). Fluorescence was detected using a FACSCalibur cytometer. A decrease in fluorescence intensity indicates a loss of mitochondrial Cytochrome C that is washed out after cell membrane permeabilization. Data analysis was performed by FlowJo 7.6 software.

2.6 Mitochondrial membrane potential ($\Delta\Psi_m$)

Analysis of $\Delta\Psi_m$ was performed in living cells with the mitochondria selective dye JC-1. Cells were harvested and incubated with JC-1 (1,25µM, 37°C, 30 minutes). Mitochondria with an intact potential display JC-1 red fluorescing aggregates, whereas in mitochondria with disrupted potential JC-1 is monomeric and green fluorescent. The shift in fluorescence was monitored by a FACSCalibur cytometer using channel FL1-H for green fluorescence. For data analysis FlowJo 7.6 software was used.

2.7 Caspase 8 activity assay

Caspase 8 activity was measured using a commercial kit (Merck Millipore, Darmstadt, Germany), based on the cleavage of a caspase-8 specific AFC (7-amino-4-trifluoromethyl coumarin) labeled peptide. Cells were harvested, washed once with ice-cold PBS and lysed by the caspase lysis buffer and stored over night at -80°C. The next day, the cell lysate was centrifuged (14,000rpm, 10min, 4°C) to remove cell debris and the supernatant was transferred to a new vial. Protein concentration was determined by Bradford assay.

For measurement 10µl of each sample was pipetted in a non-transparent 96-well plate in triplicates. 90µl of the freshly made substrate solution containing the labeled peptide was added to each well. The fluorometric shift over 5h at 37°C was monitored by a fluorescent plate reader (SpectraFluorPlus, Tecan) calculating the slope of the relative enzyme activity in %.

2.8 Isolation of mitochondria from cultured cells

A semi-automated method was used for isolating mitochondria from MDA-MB-231 cells treated with Chondramide or DMSO 0,03 % as solvent control. This assay was performed in the laboratory of Dr. Hans Zischka in collaboration with Sabine Schmitt (Institut für molekulare Toxikologie und Pharmakologie, Helmholtz Zentrum München). Briefly, cells were harvested via trypsination, counted and 5×10^6 cells were homogenized using a Balch homogenizer coupled to a high-precision pump. This method provides mitochondria from cultured cells that have a similar quality like rat liver mitochondria that resemble to be the gold standard (43). Homogenisates are subjected to two centrifugation steps (800g and 9000g) to separate the nuclei fraction (pellet 800g), the mitochondrial fraction (pellet 9000g) and the cytosolic fraction (supernatant 9000g). The mitochondrial fraction was further subjected to a protein quantification via Bradford and equal amounts of protein were used to assess the mitochondrial membrane potential via fluorescence quenching of Rhodamin123⁺ and swelling analysis at an absorbance of 540 nm. To assess a participation of the mitochondrial permeability transition pore Cyclosporin A (5 µM) and Ca²⁺ (400 µM) was added. As positive control for an intact mitochondrial membrane potential ($\Delta\Psi_m$) in control mitochondria, $\Delta\Psi_m$ was disrupted by the addition of the protonophore FCCP (Carbonyl cyanide 4(trifluoromethoxy) phenylhydrazone) (500 nm).

2.9 Western blot

2.9.1 Buffers and solutions for Western blot

Lysis buffers

Digitonin lysis buffer (pH7,2)		Phospho lysis buffer (pH 7,5)	
Mannitol	210 mM	EDTA 2xH ₂ O	2 mM
Sucrose	200 mM	NaCl	137 mM
Hepes (pH 7,2)	10 mM	Glycerol	10 %
Na ₂ EGTA	0,2 mM	Na ₄ P ₂ O ₇ x H ₂ O	2 mM
Succinate	5 mM	Tris-Base	20 mM
BSA	0,15 %	Triton X-100	1 %
Digitonin in H ₂ O	80 µg/ml	C ₃ H ₇ Na ₂ O ₆ P x H ₂ O	20 mM
		NaF	10 mM
		Na ₃ VO ₄	2 mM
		PMSF	1 mM
		Complete® mini EDTA free in H ₂ O	4 mM

Solutions for Western blot**5x SDS sample buffer**

Tris HCl (pH6,8)	3,125 mM
Glycerol	10 ml
SDS	5 %
DTT	2 %
Pyronin Y	0,0025 %
H ₂ O	

Separation gel 12 %

Polyacrylamid solution	40 %
Tris HCl pH 8,8	375 mM
SDS	0,1 %
TEMED	0,2 %
APS	0,1 %
H ₂ O	

Stacking gel

Polyacrylamid solution	40 %
Tris HCl pH 6,8	125 mM
SDS	0,1 %
TEMED	0,2 %
APS	0,1 %
H ₂ O	

Electrophoresis buffer

Tris-Base	4,9 mM
Glycine	38 mM
SDS	0,1 %
H ₂ O	

Tank buffer 5x

Tris-Base	240 mM
Glycine	195 mM
H ₂ O	

Tank buffer 1x

Tank buffer 5x	20 %
Methanol	20 %
H ₂ O	

TBS-T (pH 8,0)

Tris-Base	24,76 mM
NaCl	189,9 mM
Tween 20	0,1 %
H ₂ O	

2.9.2 Western blot, cytosolic-mitochondrial fractionation and cytosolic-cytoskeletal fractionation

The protein levels were examined by Western blotting analysis. Cells were grown in a 12-well culture dish and treated for the indicated time points. Because of dealing with cell death, the media of the cells was also collected as well as the PBS buffer which was used for washing and the T/E solution and the stopping medium. After collection cells were centrifuged at 1500 rpm for 10 minutes at 4°C and washed with PBS and transferred to an eppendorf cup. Again cells were centrifuged at 1500 rpm for 10 minutes at 4°C. Supernatant was discarded and 85µl of phospho lysis buffer was added and cells were frozen at -20°C overnight. Next day lysates were centrifuged at 10000 rpm for 10 minutes at 4°C to remove cell debris. Supernatant was collected and an aliquot was used for protein quantification via Bradford according to manufacturer's instructions. An equal amount of protein was separated via SDS-Page (100 V, 20 minutes then 200 V, 43 minutes) (Bio-Rad System, München, Germany) and transferred to a nitrocellulose membrane (GE Healthcare, München, Germany) via tank blotting (90 V for 90 minutes, 4°C). The detection of specific proteins was achieved by using the ECL WB plus reagent detection system or the Odyssey Infrared Imaging system version 2.1.

To separate the mitochondrial from the cytosolic fraction cells were harvested, incubated with the Digitonin lysis buffer (20min, on ice) and centrifuged (10min, 1,300rpm, 4°C). The supernatant was collected (cytosolic fraction) and the cell pellet was permeabilized with 0.1% TritonX-100 (15min, on ice) (mitochondrial fraction). Both fractions were centrifuged one more time (14,000rpm, 10min, 4°C) to sediment the cell debris. Mitochondrial and cytosolic fractions were then processed like Western blot lysates mentioned above.

Cytosolic and cytoskeletal fractionation was achieved by using different centrifugation steps. Cells are harvested as described above and lysed with phospho lysis buffer (30

minutes on ice). Lysates were centrifuged at 300 g for 15 minutes (4°C) to remove cell debris and keep the cytoskeletal fraction in solution. Supernatant (Cytosolic and cytoskeletal fraction) was collected and again centrifuged at 14 000 rpm for 15 minutes to separate higher molecular cytoskeletal proteins from cytosolic proteins. Supernatant containing the cytosolic fraction was carefully collected and protein content was determined via Bradford analysis. The pellet containing the cytoskeletal fraction was resolved in phospho lysis buffer and mixed with 5x SDS sample buffer. Equal amounts of protein were separated as mentioned above.

2.9.3 Primary and secondary antibodies used for immunoblotting

Primary antibodies

Antigen	Source	Dilution	In	Producer
Actin	Mouse	1:1000	Blotto 5 %	Merck-Millipore
Bad	Rabbit	1:1000	BSA 5 %	Cell Signaling Technologies
phospho-Bad (Ser112)	Mouse	1:1000	BSA 5 %	Cell Signaling Technologies
COX IV	Rabbit	1:1000	Blotto 5 %	Cell Signaling Technologies
GAPDH	Mouse	1:1000	Blotto 5 %	Santa Cruz
Hexokinase II	Rabbit	1:1000	BSA 5 %	Cell Signaling Technologies
PKC α	Rabbit	1:1000	Blotto 5 %	Santa Cruz
PKC ϵ	Rabbit	1:1000	Blotto 5 %	Santa Cruz
PARP	Rabbit	1:1000	Blotto 5 %	Cell Signaling Technologies
Pro-caspase-9	Rabbit	1:1000	Blotto 5 %	Cell Signaling Technologies
Tubulin- β	Rabbit	1:1000	BSA 5 %	Cell Signaling Technologies

Secondary antibodies

Antibody	Dilution	In	Producer
Goat-anti-mouse IgG1 HRP	1:10000	Blotto 1 %	Biozol
Goat-anti-mouse IgG HRP	1:10000	Blotto 1 %	Santa Cruz
Goat-anti-rabbit IgG HRP	1:10000	Blotto 1 %	Bio-Rad
Goat-anti-mouse IRDye® 800cw	1:20000	Blotto 1 %	Li-Cor GmbH
Goat-anti-rabbit AlexaFluor® 680	1:20000	Blotto 1 %	Molecular Probes

2.10 Transfection of FLAG.PKC ϵ and mGFP- β -actin

FLAG-PKC ϵ plasmid was a gift of Alex Toker (Addgene plasmid 10795) (63). MCF7 cells were transfected using the Amaxa Nucleofector kit V according to manufacturer's instructions. MDA-MB-231 cells were transfected using FuGene® HD transfection kit. pcDNA3.1 (Invitrogen) was used as empty vector control. Upregulation of PKC ϵ was confirmed on protein level via Western blot. 24h after transfection, cells were treated with Chondramide at indicated concentrations. For confocal microscopy MCF7 cells were transfected with mGFP- β -actin plasmid, which was a gift of Ryohei Yasuda (Addgene plasmid 21948) (64), by using the Fugene HD transfection kit according to manufacturer's instructions. mGFP- β -actin expressing cells were analyzed by confocal microscopy.

2.11 Immunostaining and confocal microscopy

To visualize a certain protein within a cell immunostaining and adjacent confocal microscopy were carried out. Cells were seeded in ibidi®-μ-slides (20000 cells/well), treated as indicated, washed with PBS⁺, fixed with 4% paraformaldehyde, permeabilized with 1% Triton-X 100 and incubated with 1% bovine-serum-albumin solution for 1 hour to block unspecific binding of antibodies. After blocking, cells were incubated with the respective antibody solution overnight (4°C), washed with PBS⁺ and incubated with the secondary antibody and a compartment selective dye for two hours. The actin cytoskeleton was either stained with f-actin selective dye Rhodamin-phalloidin or the cells were transfected with mGFP-β-actin to visualize the actin cytoskeleton. After washing with PBS⁺, stainings were sealed with mounting medium (FluorSave™ Reagent) and cover slip. Samples were kept at 4°C for longer storage. Images were obtained using a Zeiss LSM 510 META confocal microscope (Zeiss, Jena, Germany) and image analysis was performed with the Zeiss LSM image browser software.

Primary antibodies used for immunostaining

Antibody	Dilution	Producer
Bad	1:100	Cell Signaling Technologies
Hexokinase II	1:1000	Cell Signaling Technologies
PKCα	1:100	Santa Cruz
PKCε	1:100	Santa Cruz

Secondary antibodies and dyes for immunostaining

Antibody/Dye	Dilution	Producer
Alexa Fluor 488 chicken-anti-rabbit IgG	1:1000	Invitrogen
Alexa Flour 647 chicken-anti rabbit IgG	1:1000	Molecular Probes
Hoechst (bisBenzimide H 33342)	1:100	Sigma Aldrich
Mitotracker® Red CMXRos*	1:10000	Invitrogen

*Diluted in PBS⁺ and added directly to living cells (37°C, 30 Min)

2.12 Immunohistochemistry of tissue sections

Tumor and healthy breast tissues were fixed in formalin and embedded in paraffin blocks. Sections were stained with anti-PKC ϵ antibody (Santa Cruz) and visualized with the Vectastain® ABC Kit (Vector Laboratories, Burlingame, CA, USA) according to manufacturer's instructions. Four control tissues and six tumor tissues were analyzed and images were taken on an Olympus BX41 microscope with a 20-fold magnification. Tissues were provided by Dr. Doris Mayr (Pathologisches Institut, LMU München).

2.13 *In vivo* mouse xenograft model

For the subcutaneous xenograft model, 5×10^6 MDA-MB-231 cells in Matrigel/PBS (1:1) were injected subcutaneously in the flank of female SCID (C.B-17/lcrHan®Hsd-Prkdcscid, Harlan, USA) mice. 9 days after tumor cell injection, 0.75mg chondramide/kg in PBS/5% Solutol® (BASF, Ludwigshafen, Germany) was injected intraperitoneally thrice a week. After 34 days, mice were sacrificed and tumor growth and tumor weight of control (n=10) and Chondramide treated mice (n=10) was determined. Tumor volume was calculated every second day according to the formula $V = a \times b^2/2$ (a = largest side of the tumor and b = the largest side vertical to a). Average tumor volumes of the two groups were compared over time. Tumor tissues were either frozen in liquid nitrogen or fixed in formalin. Cryosections were stained for actin with rhodamine-phalloidin and anti-PKC ϵ -antibody (Abcam, Cambridge, UK) followed by incubation with anti-rabbit secondary antibody conjugated with Alexa 488 (Invitrogen). Formalin preserved sections were embedded in paraffin and stained for apoptotic cells by ApopTag® Fluorescein In Situ Apoptosis Detection Kit according to manufacturer's instructions. TUNEL positive cells were visualized with a Zeiss confocal microscope. Six randomly chosen images of each tumor were counted for TUNEL positive nuclei. All animal procedures were approved and controlled by the local ethics committee and carried out according to the guidelines of the German law of protection of animal life. The animal experiment was performed by Dr. Rebekka Kubisch and Johanna Busse in the laboratory of Prof. Dr. Ernst Wagner (Pharmaceutical Biotechnology, LMU München).

2.14 Proliferation assay

MCF7 and MDA-MB-231 cells were seeded in 96 well plates (3000 cells/well) and cultivated overnight. To detect the cell number on day 0 three wells were incubated with CellTiter-Blue® reagent for 2 hours and analyzed with a TECAN fluorescence reader according to the manufacturer's instructions to measure metabolic activity. Cells were stimulated with increasing concentrations of Dolicolide (10 - 500 nM) and DMSO 0.05% as solvent control. After 72 hours cells were incubated with CellTiter-Blue® reagent for 2 hours and measured as mentioned above. IC₅₀ values were calculated using GraphPad Prism 5.0 software non-linear regression with sigmoidal dose response.

2.15 Migration assay

To measure migration inhibition of Dolicolide on MDA-MB-231 cells xCELLigence instrument (ACEA Biosciences, San Diego, CA, USA) was used. The lower compartment of CIM-Plates® (ACEA), filled with 160 µl FCS-containing media, and the upper chamber were put together. The upper compartment was filled with 27 µl media without FCS and the plates were equilibrated at 37°C for 1 hour. MDA-MB-231 cells were harvested and resuspended in DMEM without FCS. 30000 MDA-MB-231 cells per 100 µl were added in CIM-Plates® with 8µm pore width and analyzed for 10 hours in the xCELLigence® instrument (ACEA). MDA-MB-231 cells were stimulated after adherence with the indicated concentrations of Dolicolide or DMSO 0.01% as solvent control. Data analysis was performed using RTCA 1.2.1 software (ACEA).

2.16 Statistics

The experiments were commonly performed three times in an independent manner. The statistical test used for analysis is indicated in the respective figure legend. Bars represent mean ± SEM. Statistical analysis was performed with the software GraphPad Prism Version 5.04 (GraphPad Software, Inc., La Jolla, CA, USA). Significance levels are indicated in the according figure legend.

3 RESULTS

3.1 Disrupting the actin cytoskeleton with Chondramide leads to cell death via trapping PKC ϵ

Although for Chondramide and other actin-binding compounds exist a variety of data concerning its growth inhibitory potential on different cancer cell lines (65), neither for other actin-stabilizers nor for Chondramide itself exists an explanation, how the disruption of the actin cytoskeleton leads to cell death respectively proliferation arrest (22). In this work I will show a distinct mechanism of action, how the Chondramide induced overpolymerization of the actin cytoskeleton leads to the induction of the intrinsic apoptotic pathway in breast cancer cells.

3.1.1 Chondramide impairs actin dynamics and leads to the induction of the intrinsic apoptotic pathway

3.1.1.1 FRAP-analysis of Chondramide treated cells

First, Chondramide's influence on the actin cytoskeleton should be determined. Therefore a Fluorescence-recovery after photobleaching (FRAP) assay was performed to analyze the dynamic fraction of globular actin within a cell after Chondramide treatment. A distinct region of MCF7 mammary cancer cells transfected with green fluorescent protein (GFP) tagged β -actin has been bleached by laser (488nm) and the actin filament dynamics were observed by time lapse microscopy (**Fig. 3.1 A**). Untreated cells recover from photobleaching within seconds seen by the rapid disappearance of the bleached area (**Fig. 3.1 A** upper panel, white arrows). In contrast, cells treated with 300nM Chondramide (ChA) for 30 min display a massive reduction of the mobile, globular actin fraction (**Fig. 3.1 A** lower panel, white arrows). Quantification of fluorescence recovery confirms a distinct abrogation of actin filament dynamics by ChA (**Fig. 3.1 A, graph**). Furthermore, ChA treatment time dependently induces agglomeration of globular actin which results in formation of actin lumps shown in **Fig. 3.1 B**.

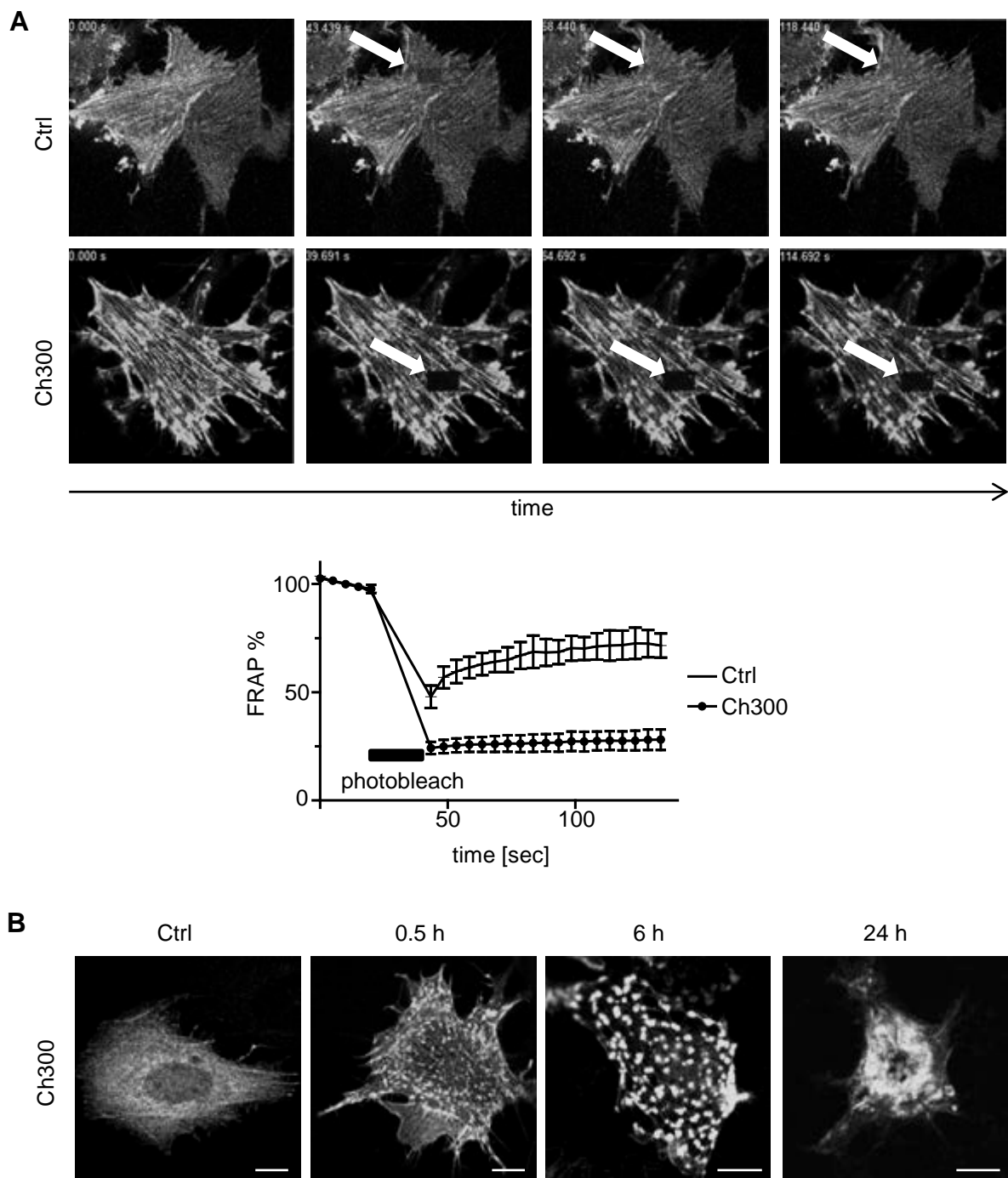


Figure 3.1: Chondramide A (ChA) inhibits actin dynamics and leads to agglomeration of actin. (A) MCF7 cells were transfected with mGFP- β -actin and treated with 300nM ChA for 30 min. The mobile actin fraction was quantified by FRAP analysis. Upper panel: White arrows indicate the photobleached area in representative images (Ctrl, untreated cells; Ch300, cells treated with 300nM ChA). Lower panel: Values represent the % fluorescence recovery over time of mGFP- β -actin after photobleach. **(B)** Time course of actin hyperpolymerization of MCF7 cells expressing mGFP- β -actin and treated with 300nM ChA (Ch300) for 0.5h, 6h and 24h. Scale bar indicates 10 μ m. n=3

Taken together Chondramide leads to a rapid overpolymerization of the actin CSK, which results in large agglomerates of actin within the cell over 24 hours.

3.1.1.2 Chondramide induces cell death in breast cancer cells

After showing the disruption of the actin CSK it was interesting to know, if such an event leads to cell death. Cell death was quantified using an Annexin-V-FITC/PI co-staining assay in MCF-7 and MDA-MB-231 cells. In both cell lines cell death was quantified to about 40 % (**Fig. 3.2**). This cell death rate aroused our interest in how exactly cell death is mediated after Chondramide treatment.

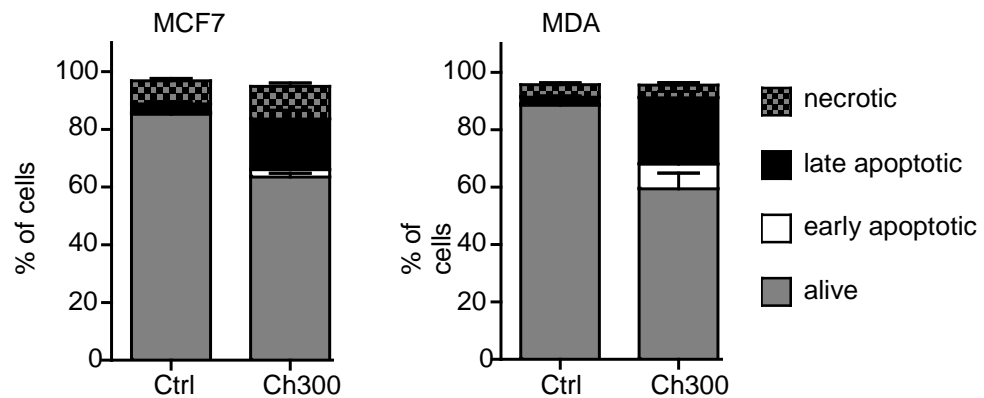


Figure 3.2: Chondramide leads to cell death in MCF7 and MDA-MB-231 cells. MCF-7 as well as MDA-MB-231 cells were treated with Chondramide (300nM, 48h) and analyzed for apoptotic cell death by staining with Annexin-V-FITC/PI. Living cells are marked in gray, early apoptotic cells in white (Annexin V positive), late apoptotic cells in black (Annexin V and PI positive) and necrotic cells in spotted gray (PI positive).

3.1.1.3 Chondramide does not influence Caspase 8 activation

One critical hallmark for the induction of the extrinsic apoptosis pathway is the activation of Caspase 8 (66). Caspase 8 activity is measured using a quenched Caspase 8 substrate that becomes fluorescent when active Caspase 8 cleaves the peptide, which can be easily monitored with a fluorescence microplate reader.

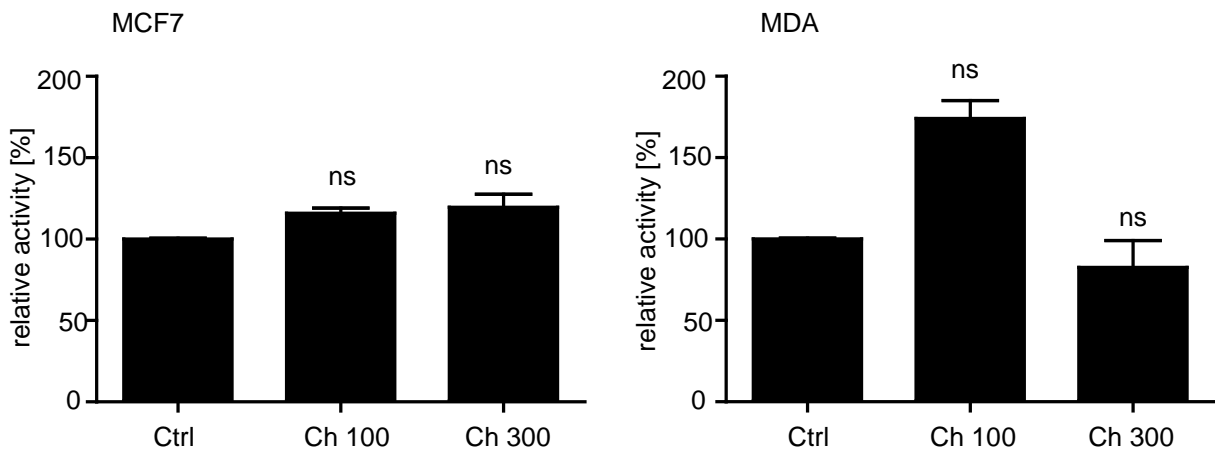


Figure 3.3: Chondramide treatment does not alter Caspase 8 activity significantly. MCF-7 and MDA-MB-231 cells were treated with 100 nM and 300 nM Chondramide for 6 hours and Caspase 8 activity was determined by the cleavage of Caspase 8 substrate Ac-Leu-Glu-Thr-Asp-AFC. Cleavage of the substrate was observed via fluorescence increase with an excitation wavelength of 390 nm and an emission wavelength of 535 nm. Bars represent the mean \pm S.E.M. ns= no statistical significant change, $p < 0,05$, (One Way ANOVA, Tuckey)

Caspase 8 activity shows no significant increase in both cell lines (**Fig. 3.3**) after 6 hours of Chondramide treatment. Especially, the apoptosis inducing concentration of 300 nM Chondramide does not alter Caspase 8 activation. These experiments make a participation of the extrinsic apoptosis pathway in Chondramide induced cell death unlikely.

3.1.1.4 Chondramide treatment leads to decrease of mitochondrial membrane potential and release of Cytochrome C from mitochondria

To further address the question, which pathway of apoptosis induction is stimulated by Chondramide treatment (intrinsic or extrinsic) we investigated the mitochondrial membrane potential ($\Delta\Psi_m$) by JC-1 iodide staining and the release of mitochondrial Cytochrome C to the cytoplasm. Both parameters are typical hallmarks of the intrinsic apoptotic pathway (29). Fluorescence profiles of both cell lines show a shift toward green fluorescence of JC-1 after Chondramide treatment indicating a decrease in mitochondrial membrane potential (**Fig. 3.4 A**). In line with disruption of mitochondrial membrane potential, Chondramide treatment (300nM) results in a release of cytochrome C from the mitochondria in both cell lines. **Fig. 3.4 B** shows FACS analysis of cytochrome C remaining in the mitochondria of cells treated with Chondramide for 24h compared to untreated cells.

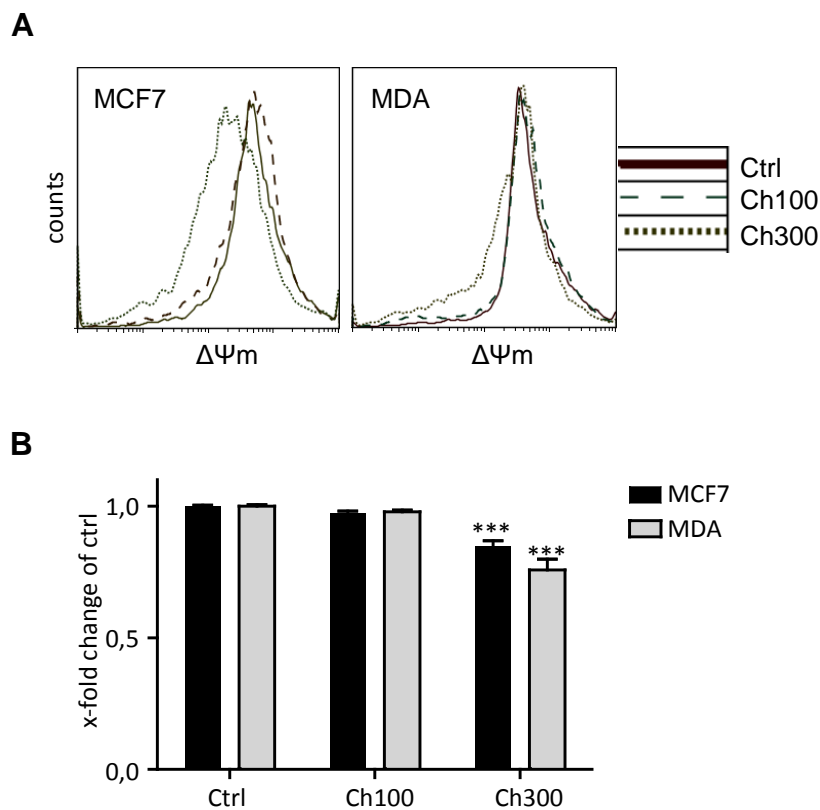


Figure 3.4: (A) Mitochondrial membrane potential ($\Delta\Psi_m$) of cells was determined by flow cytometry using JC-1 as mitochondrial selective dye. MCF7 and MDA-MB-231 cells were treated with 100nM and 300nM ChA for 24 h. (B) Mitochondrial cytochrome C content in cells (MCF7, MDA-MB-231) treated for 24h with ChA (100nM, 300nM) was measured via flow cytometry. *** $p < 0.001$ (One Way ANOVA, Bonferroni)

3.1.1.5 PARP cleavage and Caspase 9 activation by Chondramide treatment

According to the disruption of mitochondrial membrane potential and cytochrome C release also other markers of the intrinsic apoptotic pathway should be activated. Typical downstream markers for the induction of the intrinsic apoptotic pathway are the activation of caspases. We checked two caspase hallmarks: On the one hand Poly-(ADP)-ribosyl Polymerase (PARP), whose cleavage is a sign for caspase 3 activation, on the other hand pro-caspase 9, which is part of the apoptosome consisting of caspase 9, APAF-1 and cytochrome C (67). Both cell lines show a diminished expression of Procaspase 9 and a cleavage of PARP after 300 nM Chondramide treatment (**Figure 3.5**), indicating the activation of caspases 3 and 9, respectively.

In sum, our results show a disruption of the actin CSK by Chondramide and the subsequent induction of the intrinsic apoptotic pathway.

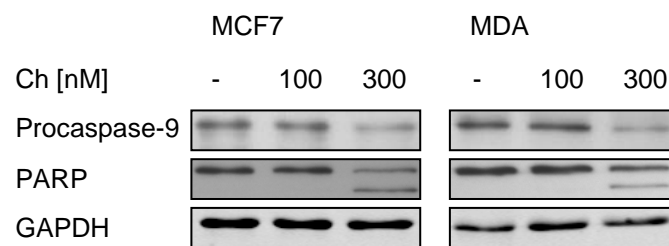


Figure 3.5: Chondramide leads to a decrease of Procaspase 9 and PARP cleavage. Western Blot analysis of procaspase-9 and cleavage of PARP as parameters for activation of caspase-9 and -3, respectively, was performed using cells exposed to ChA (100nM, 300nM, 24h). Blotting for GAPDH serves as loading control. A representative blot out of three is shown.

3.1.2 The role of mitochondrial permeability transition in Chondramide induced cell death

A crucial component of the intrinsic apoptotic pathway is the mitochondrial network. Mitochondria can be permeabilized by several molecular mechanisms (29) e.g. via the mitochondrial transition pore complex. In the following section I want to sum up the data supporting a participation of mitochondrial permeability transition (MPT) in cell death induction by Chondramide.

3.1.2.1 Chondramide induces translocation of Hexokinase II from mitochondria and dephosphorylation of Bad pointing to a role of the MPT

As Chondramide depleted mitochondrial membrane potential and induced mitochondrial cytochrome C release in mammary cancer cells, both known to be hallmarks of the mitochondrial permeability transition (MPT), we focused on major players involved in this process. VDAC, which is localized at the outer mitochondrial membrane, interacts with Hexokinase II (HKII) thereby negatively modulating MPT and preventing apoptosis. The postulated composition of the mitochondrial permeability transition complex consists, next to ANT and Cyclophilin D, also of VDAC and Hexokinase II on the cytoplasmic leaflet of the outer mitochondrial membrane (68). The association of VDAC and Hexokinase II can be analyzed indirectly via co-staining of Hexokinase II and the mitochondrial network with Mitotracker. As VDAC is one of the most abundant proteins in the outer mitochondrial membrane, it is very likely that Hexokinase II co-localizing with mitochondria is bound to VDAC. Another regulator of MPT is the proapoptotic, Bcl2-family protein Bad, which is active in a dephosphorylated status and contributes to MPT opening (45).

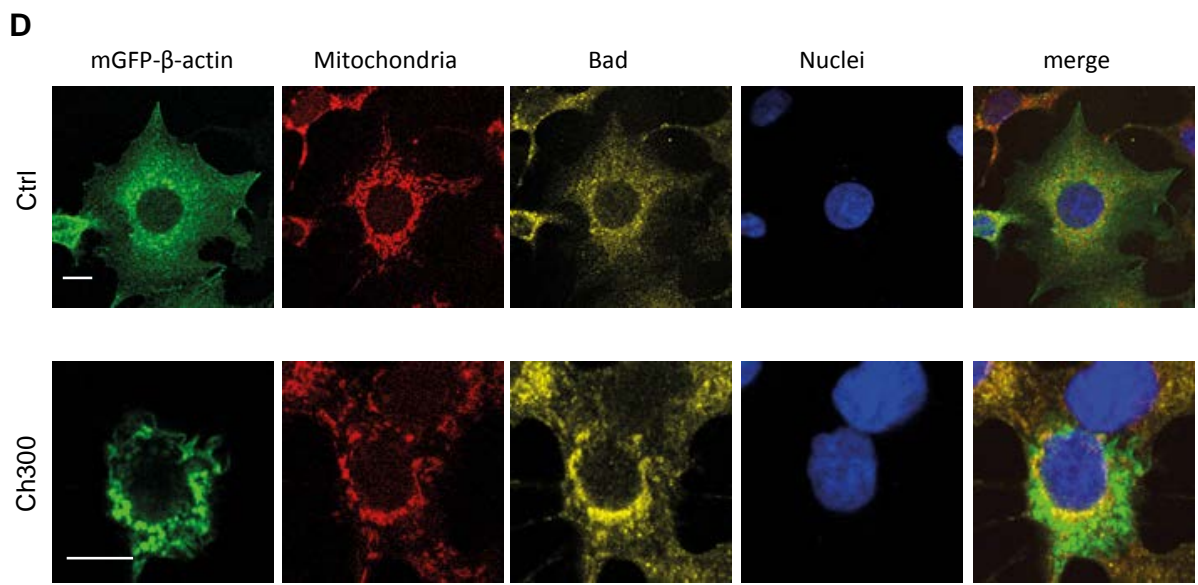
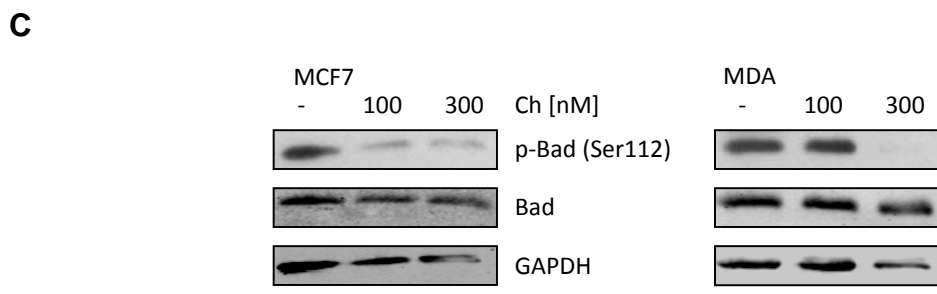
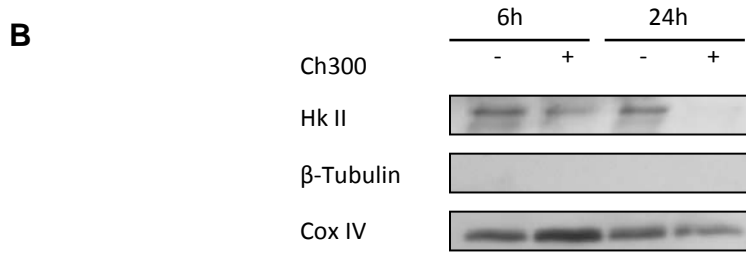
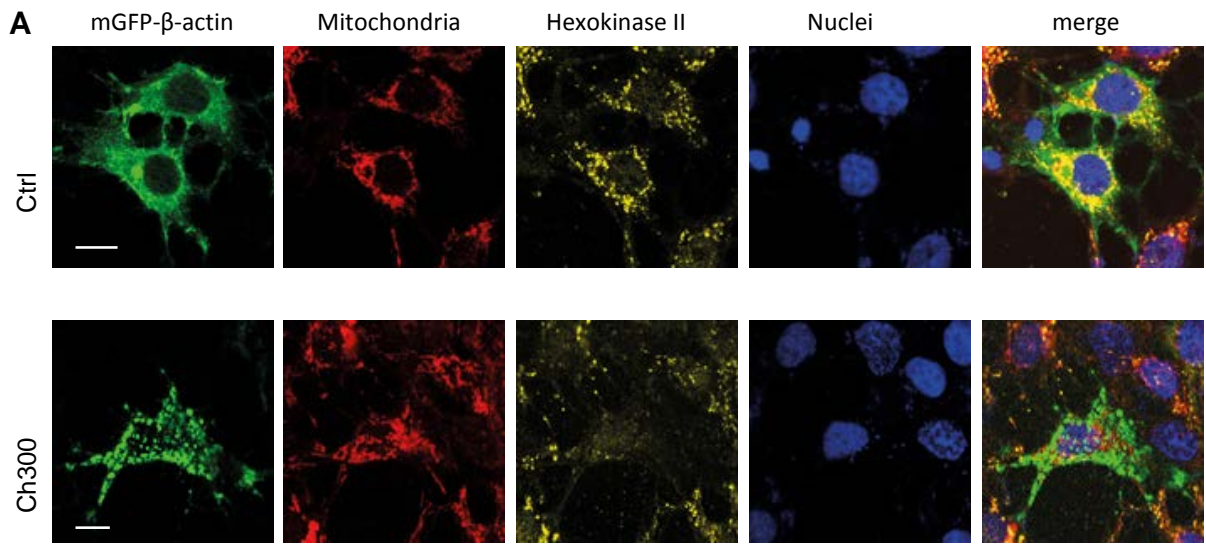


Figure 3.6: Treatment with Chondramide A leads to the dislocation of Hexokinase II (HkII) from mitochondria and activation of pro-apoptotic Bad. (A) MCF-7 cells transfected with mGFP- β -actin were treated with 300nM ChA for 6h, fixed and co-stained with Mitotracker red CMX-ROS and anti-Hexokinase II antibody followed by confocal microscopic analysis. Scale bar indicates 10 μ m. Representative images are shown. **(B)** Western Blot of HkII in mitochondrial fraction of MDA-MB-231 cells treated with 300nM ChA for 6h and 24h. Cytosolic and mitochondrial fractions were separated. Immunoblotting for β -tubulin and COX IV were used for controlling purity of mitochondrial fraction and loading control, respectively. **(C)** Western blot analysis for Bad and phospho-(Ser112)-Bad in MCF7 and MDA-MB-231 cells treated with 100nM and 300nM ChA for 6h. **(D)** MCF7 cells transfected with mGFP- β -actin were treated with 300nM ChA for 6h, fixed and co-stained with Mitotracker red CMX-ROS and anti-Bad-antibody followed by confocal microscopic analysis. Scale bar indicates 10 μ m. Representative images are shown.

We found that the binding of HkII and VDAC is impaired by Chondramide (**Fig. 3.6 A**). HkII co-localizes with mitochondria shown as a distinct dot-like pattern in control cells. In contrast, cells treated with 300nM Chondramide displayed a rather diffuse localization of HkII suggesting a disruption of the mitochondrial VDAC/HkII interaction. Western blot experiments support this notion as decreased protein levels of HkII were found in the mitochondrial fraction of cells treated with Chondramide (300nM, 6h and 24h) (**Fig. 3.6 B**).

Moreover, Chondramide affects a further regulator of the MPT, i.e. the Bcl-2 protein Bad. Protein level of Ser-112 phosphorylated, inactive Bad decreased dose-dependently after treatment of cells with Chondramide (100nM, 300nM, 6h) with constant total Bad protein (**Fig. 3.6 C**). Consequently, in cells treated with Chondramide an intensified co-localization of Bad with mitochondria was observed in comparison to untreated cells (**Fig. 3.6 D**) supporting the idea that pro-apoptotic, mitochondrial Bad is increased by Chondramide due to abrogation of the inactive, phosphorylated form of Bad.

3.1.2.2 Mitochondria of Chondramide treated cells are more sensitive towards MPT induction by Ca^{2+} implicating MPT opening

To further confirm the participation of mitochondrial permeability transition (MPT) in Chondramide induced cell death, we performed an analysis of isolated mitochondria from MDA-MB-231 cells in collaboration with the laboratory of Dr. Hans Zischka (Institute for Molecular Pharmacology and Toxicology, Helmholtz Center, Neuherberg). Importantly, Cyclosporin A efficiently blocked the Ca^{2+} -induced loss of $\Delta\Psi_m$ (**Fig. 3.7 A**) and confirms participation of the MPT in isolated mitochondria from control cells. In contrast, isolated mitochondria from ChA treated cells only weakly respond towards the inhibitory action of Cyclosporin A. A progressing depletion of $\Delta\Psi_m$ coincided with an increasing extent of mitochondria that have undergone swelling (i.e. MPT) (**Fig. 3.7 B**).

Thus, by altering known modulators of the MPT Chondramide leads to a release of Cytochrome C from mitochondria. The MPT-blocking HkII/VDAC interaction is disrupted, Bad localizes to mitochondria, and Cyclosporin A mediated inhibition of the MPT is abrogated, thus finally resulting in Cytochrome C release.

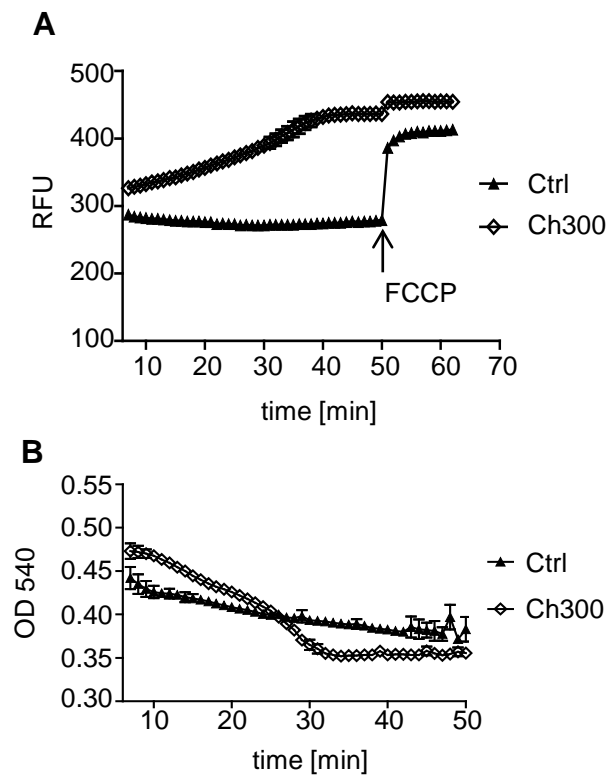


Figure 3.7: Participation of the MPT in ChA induced apoptosis. Mitochondria were isolated from either untreated (controls) or ChA treated MDA-MB-231 cells. Parallel measurements of $\Delta\Psi_m$ by Rhodamine123⁺ (125nM) quenching (A) and mitochondrial swelling (MPT) by absorbance at 540 nm (B) Mitochondria of control and ChA 300 nM (24 h) treated cells were incubated with Ca²⁺ (400 μ M) in the presence of Ciclosporin A (5 μ M). FCCP addition (500 nM) after 50 min served as internal control for $\Delta\Psi$ disruption. The experiment was independently repeated two times. These experiments were performed in collaboration with Sabine Schmitt and Dr. Hans Zischka (Institute for Molecular Pharmacology and Toxicology, Helmholtz Center, Neuherberg).

3.1.3 Chondramide inhibits PKC ϵ by trapping it in actin bundles

Ser112-phosphorylation of Bad as well as the interaction of HkII with VDAC are known to be regulated by PKC ϵ (45, 55). As PKC ϵ contains an actin-binding site our working hypothesis focused on PKC ϵ as a link between the effect of Chondramide on the actin CSK and the induction of apoptosis via mitochondrial activation. This section sets the focus on the interaction between the actin CSK and PKC ϵ and the selectivity of this interaction.

3.1.3.1 PKC ϵ colocalizes with actin bundles and is enriched in the CSK fraction under Chondramide treatment

First the interaction between the actin CSK, PKC ϵ and its Chondramide induced inclusion should be confirmed. Immunostaining of mGFP- β -actin transfected MCF7 cells showed an enrichment of PKC ϵ in Chondramide induced actin bundles 6h and 24h after treatment, indicated by the yellow color in the merged image (**Fig. 3.8 A**). Analysis of cytosolic and cytoskeletal fractions of MDA-MB-231 (**Fig. 3.8 B**) showed increased actin content in the CSK fraction after Chondramide treatment compared to control cells which, importantly, is accompanied by enhanced PKC ϵ protein levels, but not PKC α which does not contain an actin binding site.

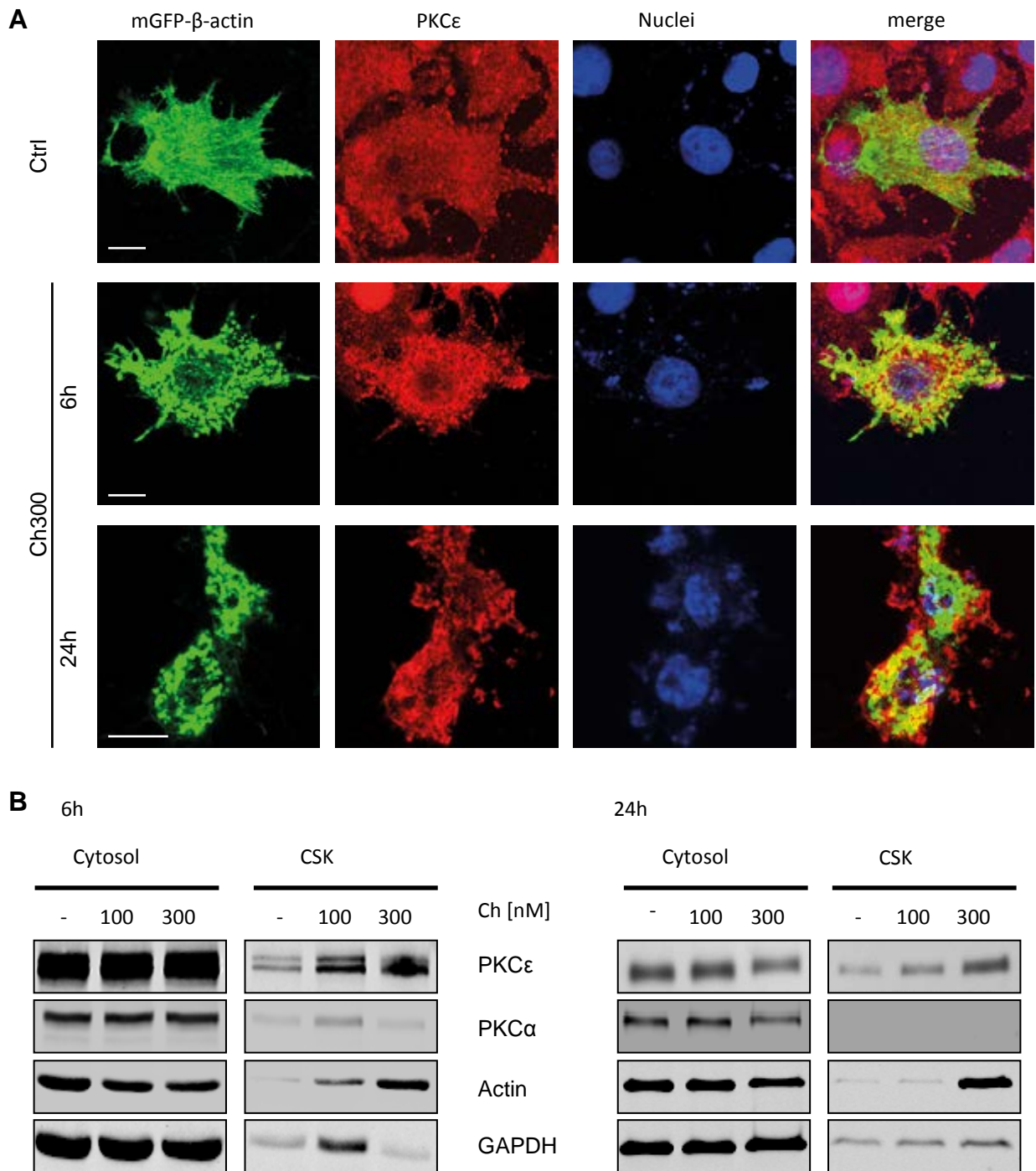


Figure 3.8: Co-localization of PKC ϵ with Chondramide induced actin bundles and its enrichment in the cytoskeletal fraction. (A) MCF7 cells were transfected with mGFP- β -actin and incubated with 300 nM ChA for 6 h and 24 h. Cells were fixed and stained for PKC ϵ . Yellow color in merged images indicates co-localization of PKC ϵ with actin bundles. Nuclei were stained by Hoechst 33342. Scale bar indicates 10 μ m. **(B)** Cytosolic and cytoskeletal fractions of MDA-MB-231 cells were isolated, resolved by SDS-PAGE and immunoblotted using antibodies against PKC α , PKC ϵ , Actin and GAPDH. Representative blots are shown.

3.1.3.2 PKC α lacking an actin-binding site does not co-localize with actin bundles

To check the specificity of the actin-binding site in PKC ϵ for its actin interaction, we also stained for another PKC isoform named PKC α , which does not contain an actin-binding site (47). PKC α does not co-localize with Chondramide induced actin bundles (**Fig. 3.9**). This supports the data from the cytosolic-cytoskeletal fractionation from **Fig. 3.8 B** and supports the notion that the interaction between PKC ϵ and the actin CSK depends on its specific actin-binding site.

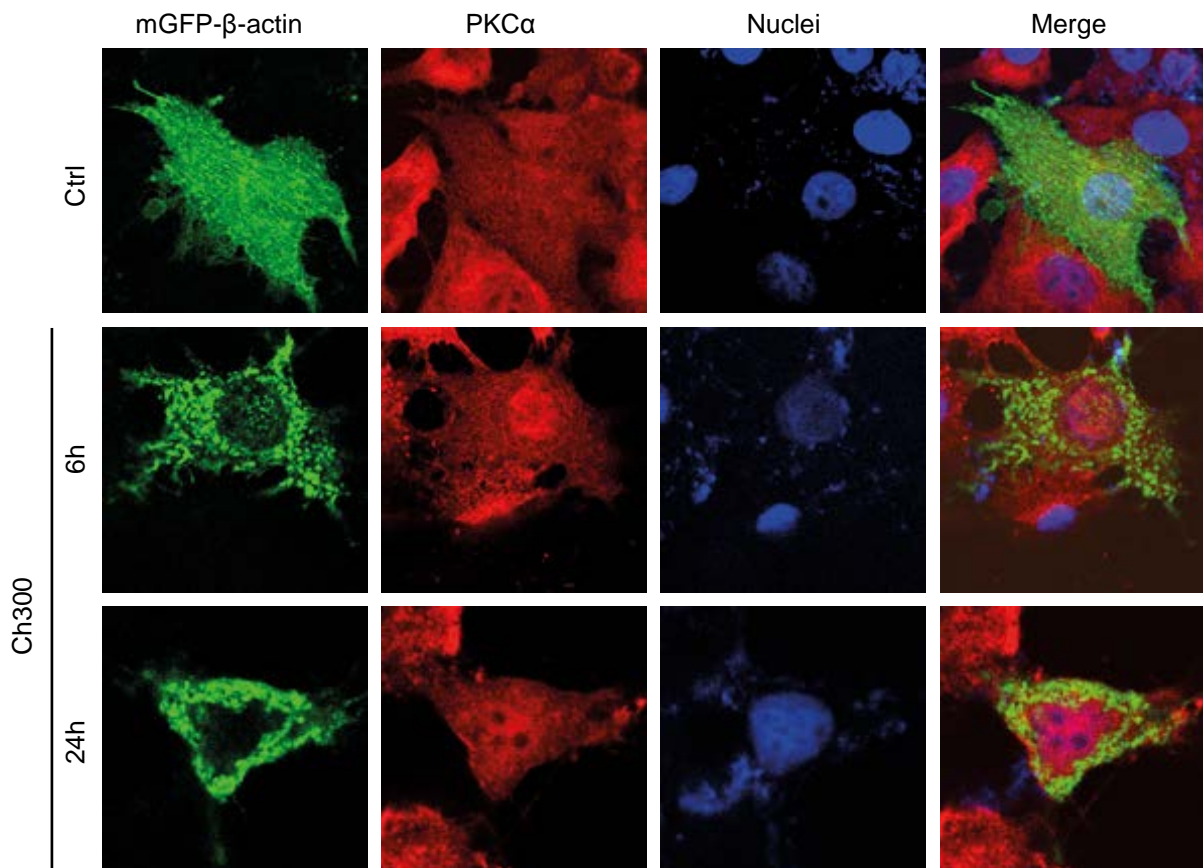


Figure 3.9: PKC α does not co-localize with Chondramide induced actin bundles. MCF7 cells transfected with mGFP- β -actin were treated with 300 nM ChA for 6 h and 24h.

3.1.3.3 Membrane localization of PKC ϵ is diminished after Chondramide treatment

After the confirmation of the co-localization of PKC ϵ and Chondramide induced actin bundles, it was also interesting to know if the activation of PKC ϵ is impaired as well. A classical marker for the activation of PKCs is its translocation to the inner leaflet of the cytoplasmic membrane after stimulation with phorbol esters (49, 52). As translocation of PKCs to the cell membrane is a typical hallmark for their activation, MDA-MB-231 cells were stained for PKC ϵ after exposure to PMA, a common inducer of PKCs (1 μ M, 30 min). PMA stimulated cells clearly display PKC ϵ protein localized on the cellular membrane, whereas additional treatment with Chondramide results in a significant decrease of PKC ϵ at the plasma membrane quantified by counting the respective cells (**Fig. 3.10**).

Taken together, the results from 3.1.3 display a trapping of PKC ϵ and impaired PKC ϵ activation as consequence of Chondramide induced polymerization of actin CSK.

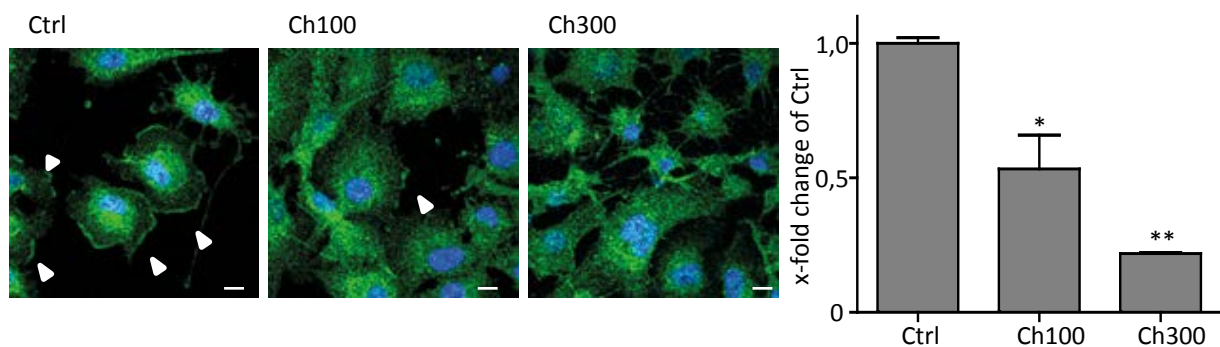


Figure 3.10: PKC ϵ shows a decreased activation after Chondramide treatment. PKC ϵ activation was determined via monitoring the translocation to the plasma membrane. MDA-MB-231 cells treated with 100 nM and 300 nM ChA for 6 h were co-stimulated with phorbol 12-myristate 13-acetate (PMA) (1 μ M, 30 min), fixed and stained for PKC ϵ . Quantification of cells with activated PKC ϵ was done by analyzing at least 80 cells per group for their PKC ϵ membrane localization (confocal microscopy). Shown are representative images, white arrows indicate cells with active PKC ϵ . Scale bar indicates 10 μ m. The graph shows a normalized statistical analysis. Bars represent the mean \pm S.E.M. of three independent experiments performed in triplicates, * $p < 0.05$, ** $p < 0.01$ (One Way ANOVA, Bonferroni)

3.1.4 PKC ϵ overexpression leads to cell death reduction

Our next aim was to verify the crucial role of PKC ϵ in cell death induction by Chondramide. Therefore overexpression of PKC ϵ protein levels might overcome the trapping of PKC ϵ in actin bundles and sustain PKC ϵ survival signaling. In order to prove the link between PKC ϵ and Chondramide induced apoptosis, cells overexpressing PKC ϵ were analyzed for their apoptotic response upon Chondramide treatment (**Fig. 3.11**). Overexpression of PKC ϵ was verified by Western blot analysis (Insets; **Fig. 3.11**). PKC ϵ transfected MCF7 and MDA-MB-231 cells show a significant decrease in sensitivity towards Chondramide treatment compared to cells transfected with empty vector plasmid, thus verifying the importance of PKC ϵ in cell death induction mediated by Chondramide.

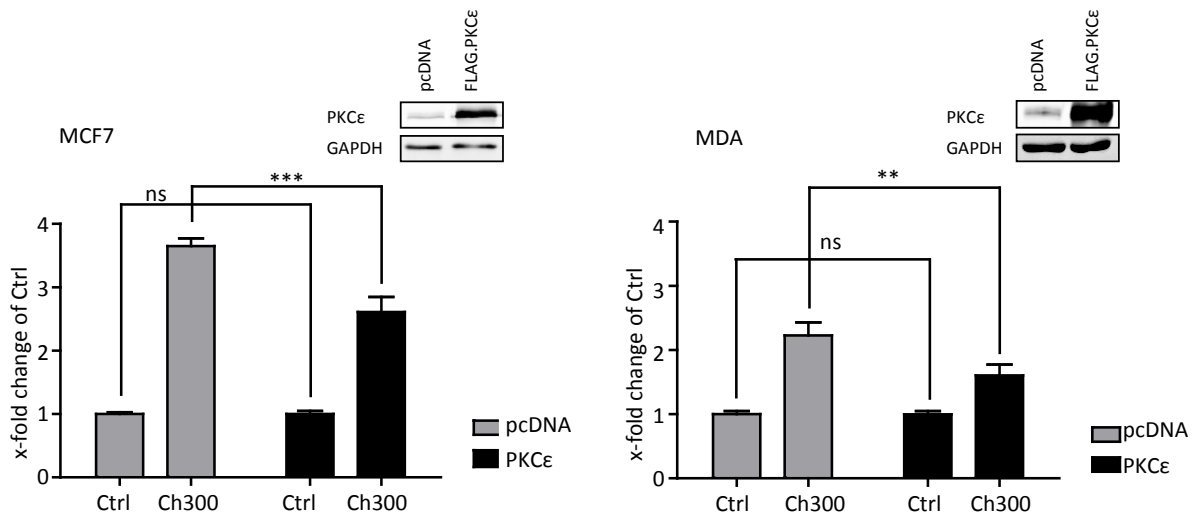


Figure 3.11: PKC ϵ overexpression rescues cells from Chondramide induced apoptosis. MCF7 and MDA-MB-231 cells were transfected with FLAG.PKC ϵ or an empty vector and treated with 300nM ChA for 24 h. The number of dead cells was analyzed using the propidium iodide exclusion assay for MCF7 cells and Annexin V staining for MDA-MB-231 cells. Overexpression of PKC ϵ was confirmed by Western Blot (Insets). The graphs show the results normalized to the according control. ns no significant difference, ** $p < 0,01$; *** $p < 0,001$ (One-Way-ANOVA, Bonferroni)

3.1.5 Chondramide treatment displays tumor cell specificity

3.1.5.1 Non-tumor cells express lower levels of PKC ϵ and are not prone to cell death towards Chondramide treatment

The distinct role of PKC ϵ in Chondramide induced cancer cell apoptosis and even more its selectivity towards tumor cells was demonstrated by another set of experiments. The effect of Chondramide on the two tumor cell lines (MCF-7, MDA-MB-231) was compared to that on the non-tumorigenic breast epithelial cell line MCF10-A (**Fig. 3.12**). Treatment with 300nM Chondramide disrupts the actin CSK in MCF10-A as well (**Fig. 3.12 A**), however MCF10-A cells show no increased cell death rate in contrast to MCF7 and MDA-MB-231 cells after stimulation with Chondramide (**Fig. 3.12 B**). To link PKC ϵ to induction of apoptosis we compared PKC ϵ protein levels in all three cell lines. Of note, MCF10-A non-tumorigenic cells express much less PKC ϵ protein than MCF7 and MDA-MB-231 cancer cells (**Fig. 3.12 C**). A similar picture was observed when analyzing breast tissue from patients (obtained from Doris Mayr, Institute for Pathology, LMU Munich). Human breast cancer tissues display a massive expression of PKC ϵ whereas healthy breast tissues show only weak staining for PKC ϵ besides in acini of breast glandular cells (**Fig. 3.12 D**).

In sum Chondramide induced apoptosis is mediated by actin CSK disruption and is highly depending on the expression of PKC ϵ in cells.

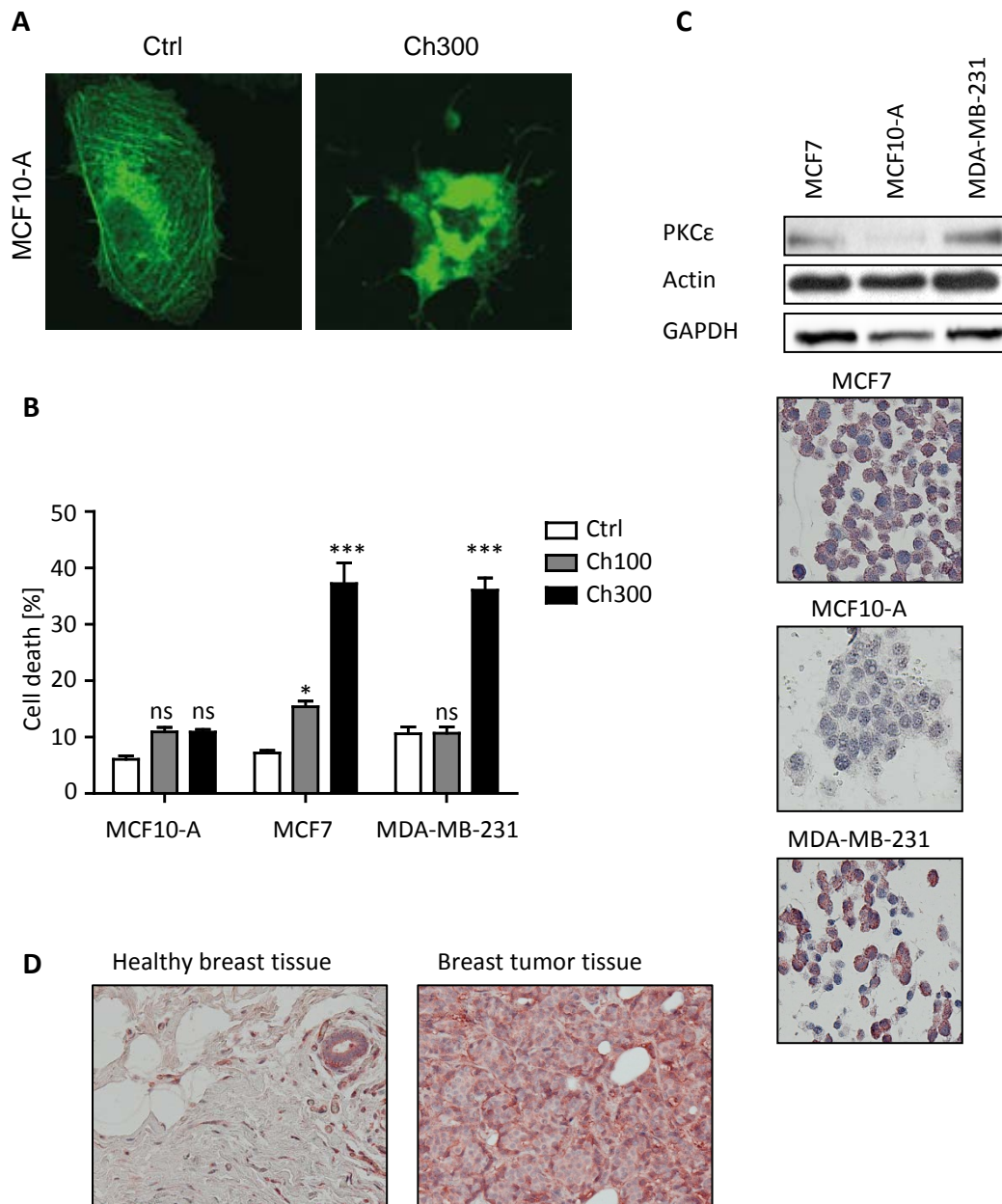


Figure 3.12: Non-cancerous cells are less susceptible to Chondramide, though the actin CSK is also disrupted. (A) MCF10-A cells were transfected with mGFP-actin and treated with 300 nM Chondramide for 24h. **(B)** The adenocarcinoma cell lines MCF7, MDA-MB-231 and the non-tumorigenic epithelial breast cell line MCF10-A were evaluated for their responsiveness to Chondramide by monitoring PI positive cells. **(C)** Comparison of PKCε levels is shown in MCF7, MDA-MB-231 and MCF10-A via Western blot as well as via immunohistochemistry. GAPDH and actin serve as loading control. Each experiment was independently performed three times. **(D)** Representative PKCε tissue stainings of healthy breast tissue and mammary tumor tissue. Nuclei are counterstained with Hematoxylin. * $p < 0.05$, ** $p < 0.01$, *** $p < 0.001$ (One Way ANOVA, Bonferroni). Confocal images, cell death quantification and Western blot analysis were conducted by Christina Moser.

3.1.6 Chondramide has anti-tumor effects *in vivo*

To prove the feasibility of Chondramide as potential anti-cancer treatment an ectopic breast cancer model was used to address this question. This animal experiment was conducted by Johanna Busse and Rebekka Kubisch from the laboratory of Prof. Ernst Wagner (Pharmaceutical Biotechnology, Ludwig-Maximilians-University, Munich).

3.1.6.1 Chondramide treatment reduces tumor growth and increases apoptotic cell death *in vivo*

Using a MDA-MB-231 xenograft mouse model administration of 0.75mg/kg Chondramide (three times per week) was shown to significantly reduce tumor growth as monitored by tumor volume (**Fig. 3.13 A**). Tumor tissue was examined for apoptotic cells (TUNEL assay) and showed a significant increase of apoptotic nuclei in the Chondramide treated group compared to control tissue (**Fig. 3.13 B**). Furthermore, the mouse body weight was measured during the treatment period and no significant difference between the Chondramide treated group and the control group was observable indicating tolerable adverse effects of Chondramide treatment (**Fig. 3.13 C**).

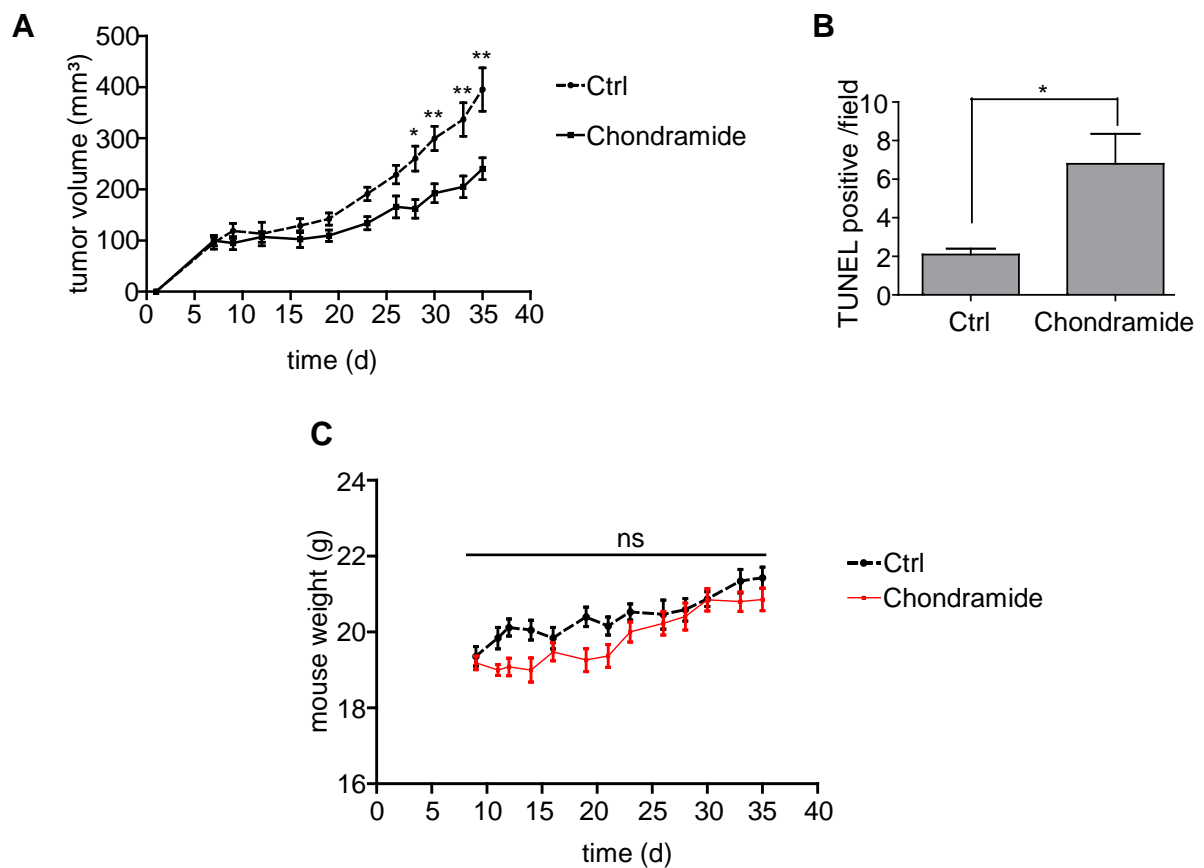


Figure 3.13: Chondramide treatment decreases tumor growth, increases apoptotic cell death, but has no influence on mouse body weight. (A) Tumor volume of female SCID mice harboring a MDA-MB-231 tumor in their flank that were either treated with solvent control (DMSO) or 0.75mg/kg/day Chondramide. **(B)** Statistical analysis of TUNEL stained paraffin sections. Six fields per tumor were visualized and counted. Significance analysis was performed using student-t-test with * $p < 0.05$, ** $p < 0.01$. **(C)** Body weight of female SCID mice during the treatment period normalized to day 7 after tumor inoculation (start of treatment).

3.1.6.2 Chondramide leads to actin clumping and PKC ϵ trapping *in vivo*

Next to standard examinations like TUNEL analysis, cryosections of the tumor tissue were investigated, in order to detect similar actin perturbations like in the cell culture model. Also the interaction between the actin CSK and PKC ϵ was analyzed *in vivo*. Chondramide leads also *in vivo* to a disruption of actin cytoskeleton (especially on the border of tumors) and moreover, PKC ϵ is localized in actin bundles in Chondramide treated tumors (**Fig. 3.14**).

In sum this set of experiments shown in 3.1.6 confirms Chondramides' cell death inducing mechanism *in vivo* and proves the feasibility of actin targeting in an ectopic tumor model.

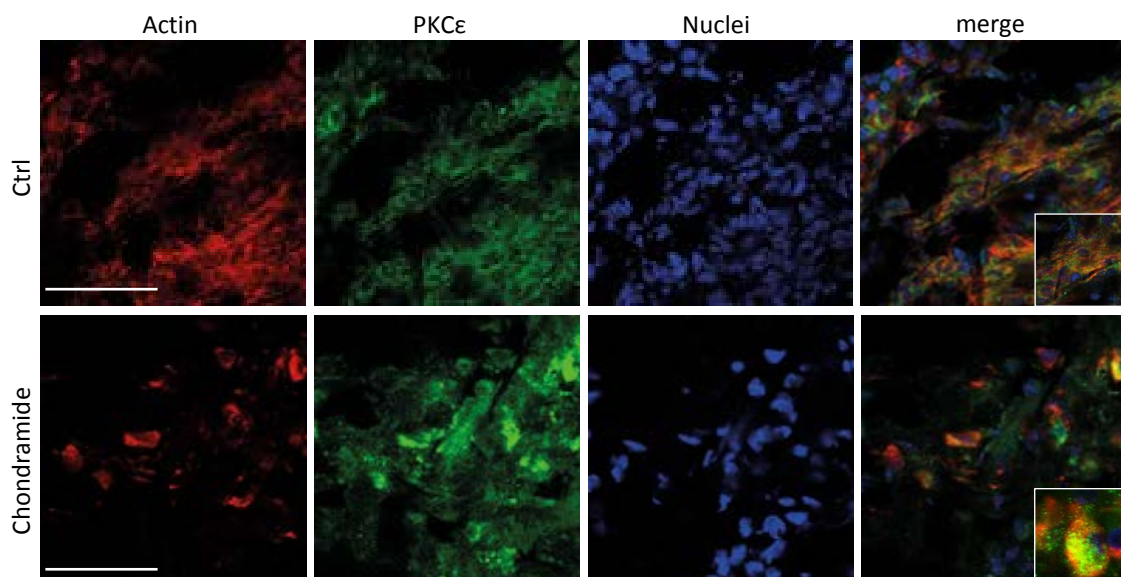


Figure 3.14: Chondramide induces actin polymerization and trapping of PKC ϵ *in vivo*. Cryosections of tumors were stained for actin (red), PKC ϵ (green) and nuclei (blue). Scale bar indicates 50 μ m. Representative images of control and Chondramide treated tumor borders are shown. Inserts in the merged images show a magnification of a few single cells. 5 tissue sections of control and Chondramide treated tumors were investigated.

3.2 Characterization of actin-binding Dolicolide in breast cancer cells

Similar to Chondramide also Dolicolide is known to bind to the actin CSK and to overpolymerize it (69). But no closer characterization of Dolicolides' action in cancer cells is available in literature. In the following section basic effects of Dolicolide on breast cancer cells will be provided.

3.2.1 Effects of Dolicolide on the actin cytoskeleton

First, we wanted to examine the effects of Dolicolide on the actin cytoskeleton of breast cancer cells. This was achieved by two means: one via a FRAP-assay to determine early effects and rhodamine-phalloidin staining to detect later effects on the actin cytoskeleton. We analyzed the short-term effects of Dolicolide on the actin cytoskeleton in GFP-tagged β -actin transfected MCF7 cells via fluorescence recovery after photobleach (FRAP) analysis (**Fig. 3.15 A**). Green fluorescent MCF7 cells were randomly chosen and a Region of Interest (ROI) of similar size was determined. This area was bleached by high laser energy (488 nm) and the fluorescence intensity was measured every two seconds. In control cells the bleached area was rapidly refilled by diffusing g-actin monomers. Cells treated with 100 nM Dolicolide for 30 minutes showed a slower fluorescence recovery over time, whereas cells treated with 300 nM Dolicolide showed no more fluorescence recovery at all indicating that g-actin monomers were reduced by Dolicolide treatment. The quantification of control cells and 300 nM Dolicolide treated MCF7 cells is shown in **Fig. 3.15 B**. The difference in fluorescence intensity after photobleaching between control and treated cells can be explained by the very fast re-diffusion of g-actin monomers into the bleached area during the process of image generation (two seconds). **Fig. 3.15 C** shows long term effects (24 hours) of Dolicolide treatment on the actin cytoskeleton of MCF7 and MDA-MB-231 cells. 100 nM Dolicolide lead to reduced actin stress-fibers compared to control cells. 300 nM and 500 nM Dolicolide show effects on the formation of actin bundles in both cell lines.

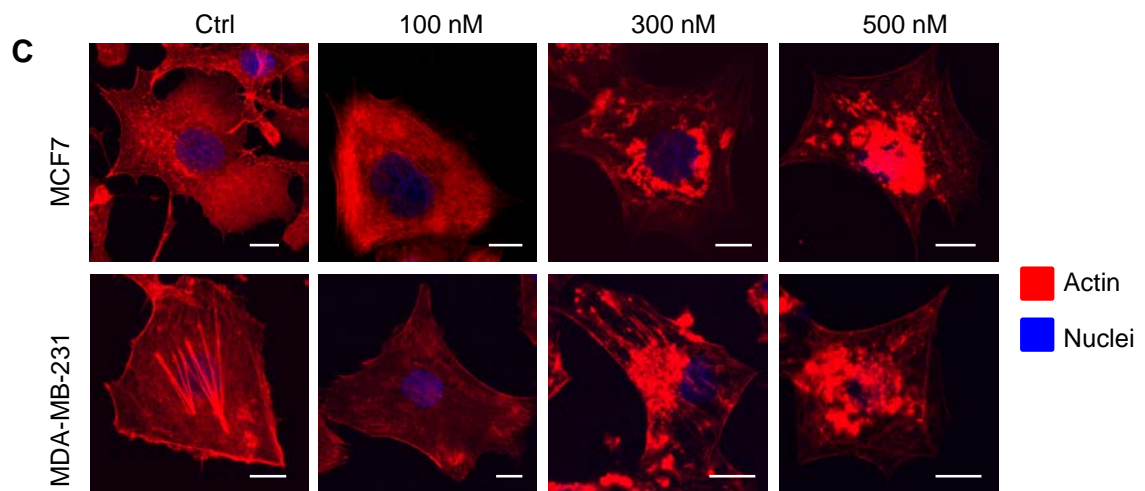
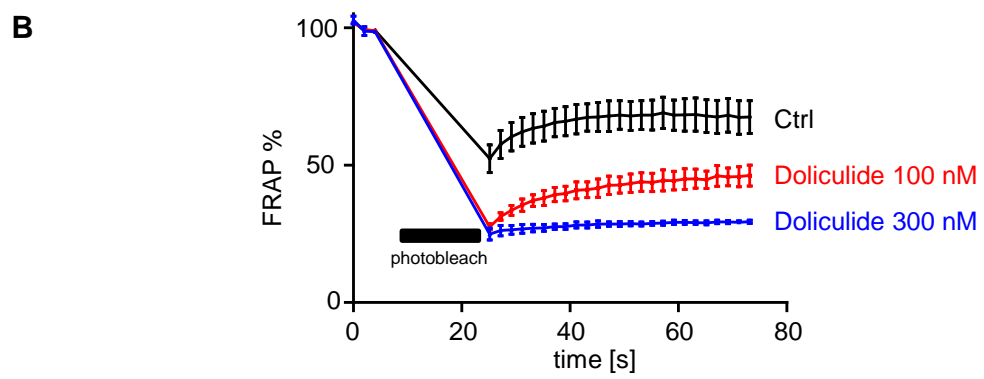
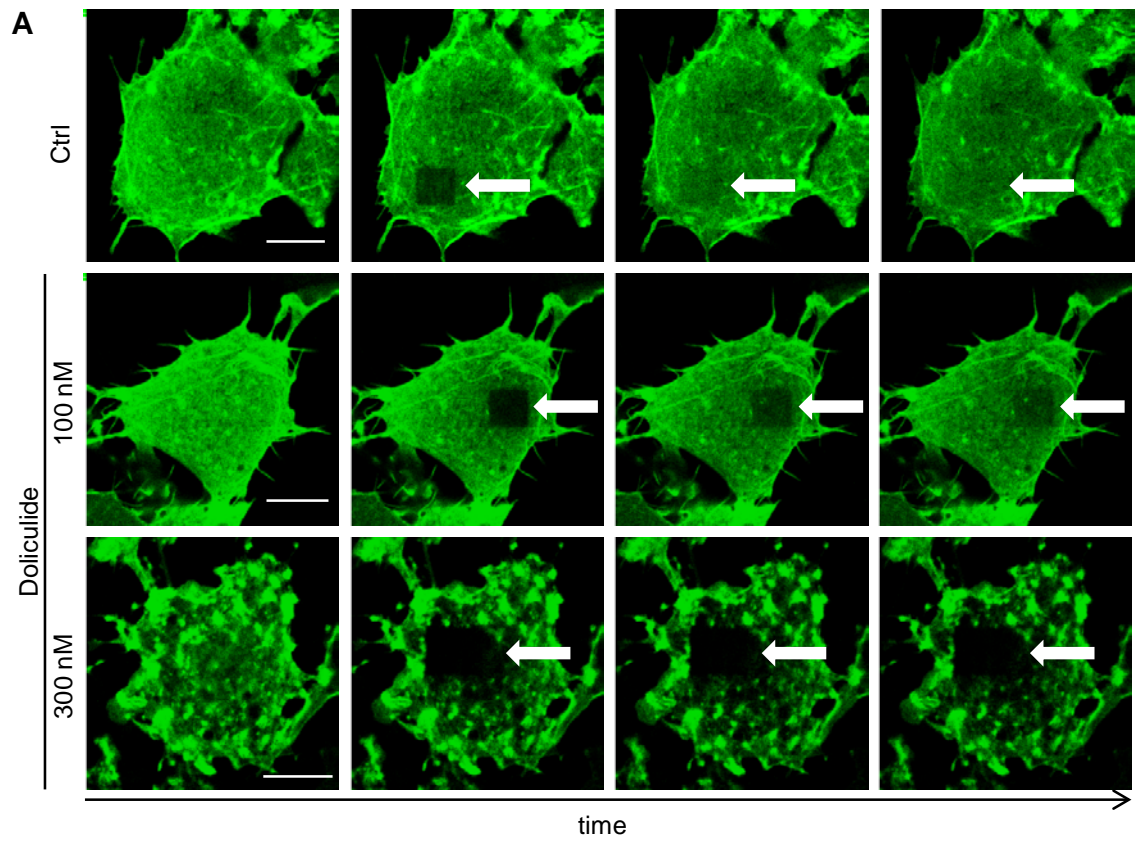


Figure 3.15: Dolicolide inhibits actin dynamics and leads to the formation of actin bundles. (A) Fluorescence recovery after photobleach (FRAP) analysis of MCF7 cells. MCF7 cells were transfected with mGFP- β -actin and treated with 100 nM and 300 nM Dolicolide for 30 min. The mobile actin fraction was quantified by FRAP analysis. White arrows indicate the photobleached area in representative images. (B) Values represent the % fluorescence recovery over time of mGFP- β -actin after photobleach of control and 300 nM Dolicolide treated cells. (C) Actin staining of MCF7 and MDA-MB-231 cells by rhodamin-phalloidin. Cells were treated for 24 hours with 100 nM, 300 nM and 500 nM Dolicolide and stained for filamentous actin (red) and nuclei (blue). Scale bar indicates 10 μ m. Each experiment was performed independently three times.

3.2.2 Effects of Dolicolide on functional parameters of breast cancer cells

The next aim was to investigate Dolicolide's impact on a functional level of breast cancer cells like proliferation of MCF-7 and MDA-MB-231 cells as well as migration of the invasive breast cancer cell line MDA-MB-231. As shown in **Fig. 3.16 A** Dolicolide inhibits proliferation dose-dependently after 72 hours in MCF7 and MDA-MB-231 with an IC_{50} of 93 nM and 77 nM, respectively. The influence on migration by Dolicolide was tested in highly metastatic MDA-MB-231 cells (**Fig. 3.16 B**). The migratory potential of MDA-MB-231 was analyzed for eight hours by impedance measurements (xCELLigence), revealing a dose-dependent inhibition of migration by Dolicolide treatment compared to control cells. The negative control, containing no FCS in the lower compartment of the CIM-Plate® does not migrate at all.

In sum, Dolicolide impairs crucial characteristics of malignant breast cancer cells, namely proliferation and migration.

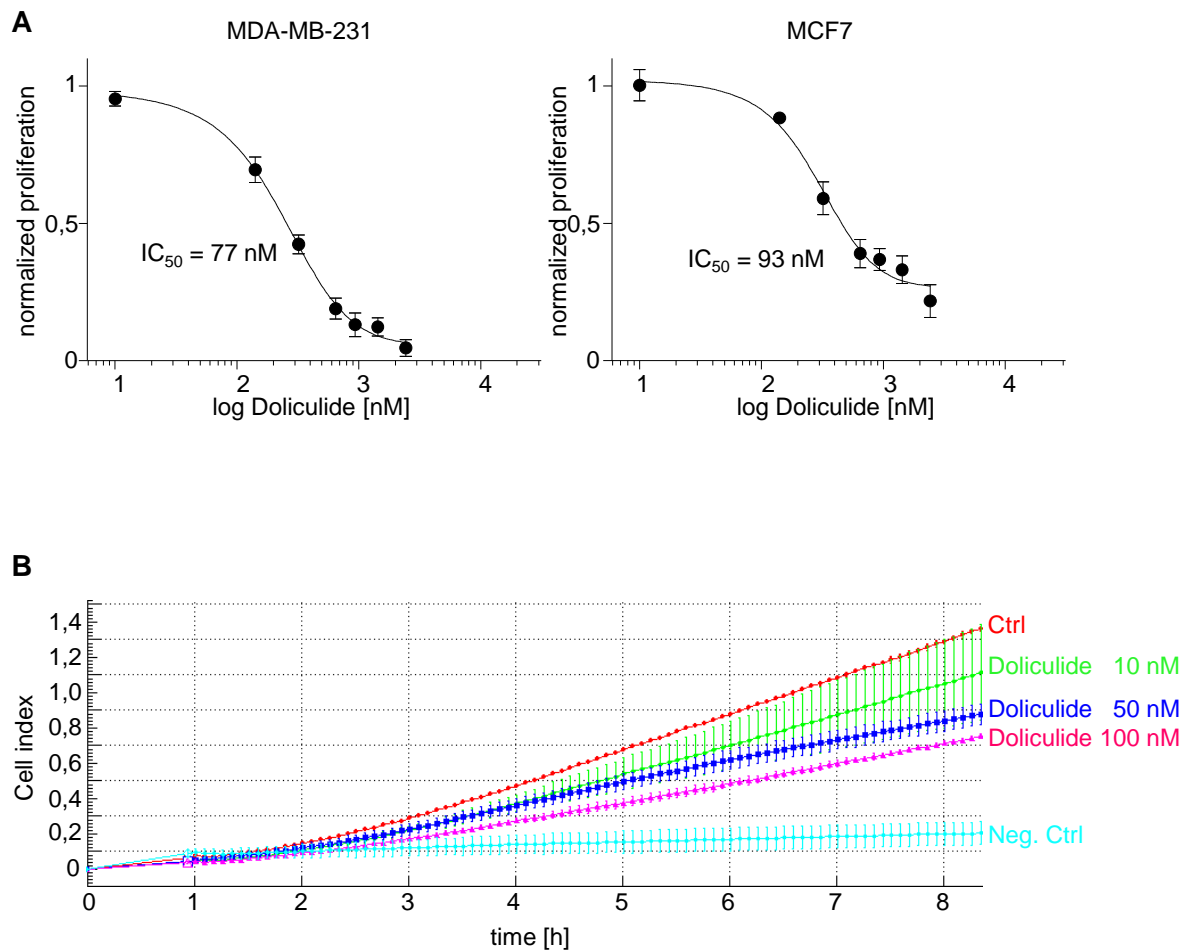


Figure 3.16: Dolicolide inhibits proliferation and impairs migration of invasive breast cancer cells. (A) Logarithmical proliferation of MCF7 and MDA-MB-231 cells determined via CellTiter-Blue® assay. Cells were treated for 72 hours with increasing Dolicolide concentrations (10, 50, 100, 150, 200, 300 and 500 nM) and 0.05% DMSO as solvent control. IC_{50} values indicate the Dolicolide concentration when the proliferation inhibition is half maximum. **(B)** Transwell migration assay with MDA-MB-231 cells. MDA-MB-231 cells were treated with subtoxic Dolicolide concentrations (10, 50 and 100 nM) for 8 hours and migration through a 8 μm pore-size membrane was detected using the xCELLigence® impedance measurement device. Negative control contained no chemo-attractant in the lower compartment.

3.2.3 Dolicolide induces apoptosis

Another typical hallmark of cancer cells is their capability to evade apoptosis (30). In this section we determined Dolicolides' potential to induce apoptosis in breast cancer cells. Cell death was quantified with propidium iodide exclusion assay in MCF7 and MDA-MB-231 cells (**Fig. 3.18 A**). Both cell lines show an increased rate of PI positive cells after 24 hours Dolicolide exposure in a dose-dependent manner. Western blot analysis of MCF7 and MDA-MB-231 cells shows classical apoptotic marker proteins Pro-caspase 9 and Poly-(ADP)-ribonucleotid-Polymerase (PARP) (**Fig. 3.18 B**). Dolicolide leads to a dose-dependent decrease of Pro-caspase 9 pointing to its activation. In addition, PARP cleavage is strongly induced in Dolicolide treated cells indicating activation of caspase-3 thus confirming the induction of apoptosis.

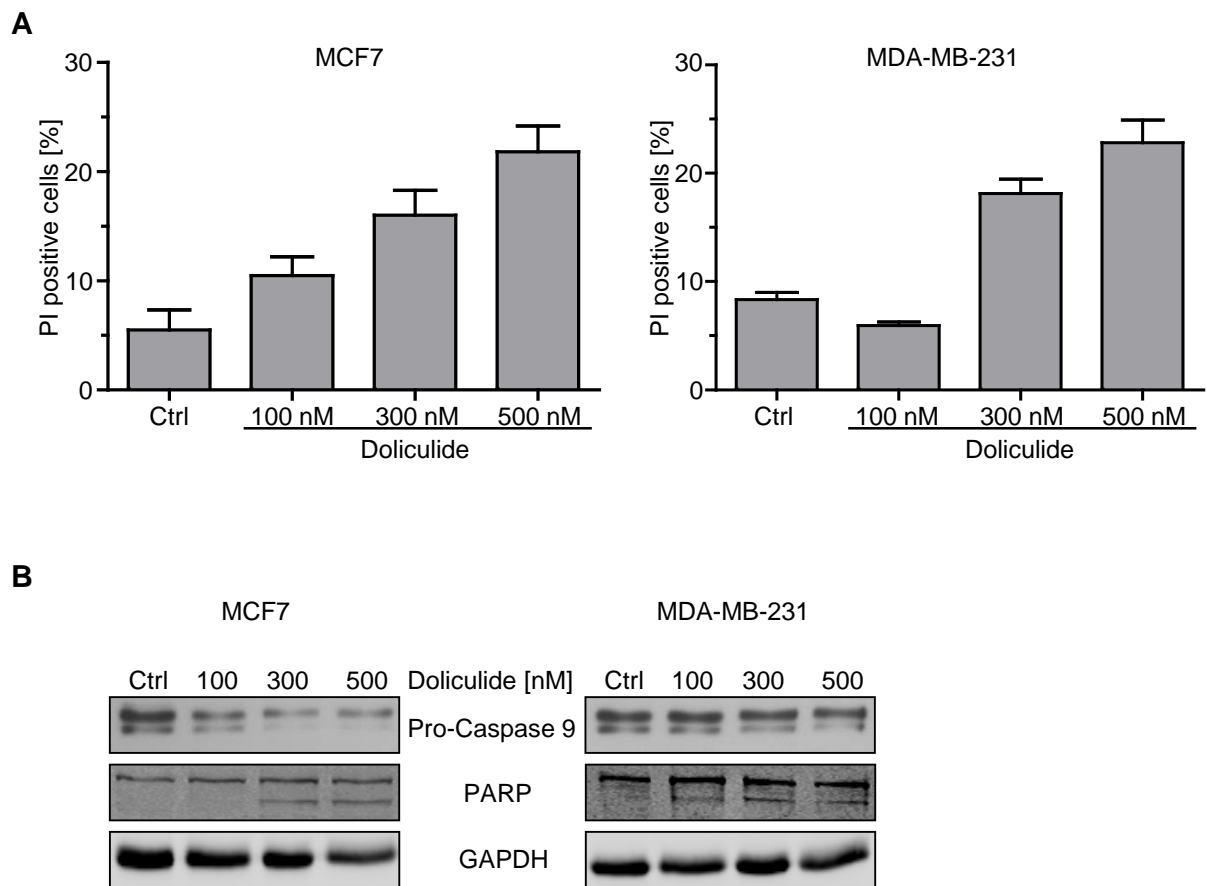


Figure 3.18: Dolicolide induces cell death and leads to caspase activation and PARP cleavage. (A) Propidium iodide exclusion assay of MCF7 and MDA-MB-231 cells treated with 100 nM, 300 nM and 500 nM Dolicolide for 24 hours. (B) Western blot analysis of apoptotic marker proteins Pro-caspase 9 and PARP in MCF7 and MDA-MB-231 cells treated with 100 nM, 300 nM and 500 nM Dolicolide for 48 hours. GAPDH serves as loading control. A representative blot out of three is shown.

Taken together, we could show that Dolicolide leads to the overpolymerization of the actin CSK, inhibition of functional cancer characteristics and the induction of apoptosis.

4 DISCUSSION

The actin and microtubule cytoskeletons play pivotal roles in cancer biology as they regulate tumor relevant processes for example cell cycle, morphogenesis or migration. Actin fulfills multiple functions in eukaryotic cells like movement of intracellular organelles, migration of the cell, and separation of the cell bodies in the end of mitosis (70). The actin cytoskeleton (CSK) is a tightly regulated network of globular actin monomers that ATP-dependently polymerize into complex structures (26). Concerning their special duties in cell movements, actin filaments are polarized with barbed and pointed ends, because the actin monomers always interact in the same direction, which leads to the polarization of the filaments. The assembly, elongation and dissociation of actin monomers to filaments are highly regulated mechanisms, which involve more than 100 actin-related proteins (23). Moreover, the equilibrium between monomeric and filamentous actin can also be affected by natural compounds, which arose in a broad variety in several species like marine organisms, fungi and myxobacteria. These compounds can be divided into two mechanistically different groups: compounds that inhibit filament assembly or depolymerize filaments like Latrunculin B and Cytochalasin D and those that stabilize or overpolymerize the actin CSK like Chondramide, Jasplakinolide or Phalloidin (12, 16, 20).

Another main component of the CSK are the microtubules, building up the microtubule network that regulates the transport of organelles and is an important structure in the mitotic spindle apparatus responsible for the segregation of chromosomes during mitosis (71). To date, a wide range of natural compounds is available, which overpolymerize or depolymerize the microtubule CSK and lead to cell death in cancer cells. Notably, contrary to actin binding compounds several of these natural products or synthetic derivatives of them are in clinical use as anti-cancer agents for decades, like the Taxanes, Epothilones or Vinca alkaloids (72). One reason for the extensive use of microtubule targeting drugs in cancer treatments might be their very well understood mechanism of action (73, 74). In contrast, the pharmacological properties of actin-binding compounds are so far poorly described (22). This is the reason why we used Chondramide A and Dolicolide as tools to decipher the mechanisms behind their anti-cancer actions.

4.1 Targeting the actin cytoskeleton with Chondramide A: selective anti-tumor action via trapping PKC ϵ

The data communicated here provide a conceptual framework for actin-polymerizing agents such as Chondramide as tumor cell specific, cytotoxic drugs. Major findings were: 1) The actin cytoskeleton is involved in specific apoptotic signaling via PKC ϵ and regulation of mitochondrial permeability transition (MPT). As PKC ϵ is overexpressed in

cancer cells a tumor cell selective mode of action is proposed. 2) Actin-targeting Chondramide masters the challenge of isoform specific inhibition of PKC, namely protumorigenic PKC ϵ . 3) Chondramide induces apoptosis and displays *in vivo* efficacy via disruption of PKC ϵ signaling.

4.1.1 PKC ϵ is an interesting candidate linking the actin CSK to cell death

Pharmacological interruption of actin dynamics has been reported before to lead to cell death however the exact mechanisms remain unclear (22). Posey et al. hypothesized a role of gelsolin, an actin binding protein, for apoptosis induced by another actin polymerizing natural compound named Jasplakinolide, however gelsolin overexpression was shown to have no impact on apoptosis induction by Jasplakinolide (75). We used Chondramide as a chemical tool to learn more about actin specific apoptotic signaling. Chondramide, similar to Jasplakinolide (76), hyperpolymerizes the actin cytoskeleton, induces agglomeration of actin that assembles over time and forms massive amorphous actin bundles which contain actin-binding proteins as reported (77). Our driving strategy was to search for regulators of cell death containing an actin-binding site and to examine whether they might be trapped within these actin structures and thereby display decreased functionality. We came up with PKC ϵ , a member of the PKC family, which on one hand possesses an actin-binding motif (49, 78) and is on the other hand a crucial regulator of several pro-survival pathways (50, 52, 59-62).

4.1.2 PKC ϵ is the “Bad guy” among PKCs

The PKC family has been an exciting target for drug discovery especially in cancer ever since they were identified as intracellular receptors for the tumor promoting agents phorbol esters (79). However, major challenges such as dissecting the contribution of PKC isozymes to cancer progression or developing modulators specific for the PKC isozymes are still to be met. PKCs are either pro-mitogenic or inhibit cell-cycle progression depending on isozyme and cell type. PKC α and PKC δ for instance promote anti-mitotic responses (80) in tumor cells whereas PKC ϵ is required for cancer cell survival (50, 52). Further, PKC ϵ has been shown to be overexpressed in various types of cancer including breast cancer (60, 62) supported by our own data.

4.1.3 Apoptosis via MPT is modulated by PKC ϵ and affected by Chondramide

PKC ϵ mediates oncogenic activities as it affects the activity of transcription factors like ATF2, NF κ B and Stat3 (51, 55, 81), but also addresses distinct targets in the apoptotic machinery of cells such as the BH3-only Bcl2-family protein Bad. Bad exerts its pro-apoptotic functions in a dephosphorylated form and PKC ϵ is known to directly phosphorylate Bad on Serine 112, thus inhibiting the pro-apoptotic activity of Bad (45, 56, 82) by preventing the mitochondrial permeability transition (MPT) (45) and hence the onset of apoptosis. PKC ϵ counteracts the MPT not only via inactivation of Bad but also by maintaining the complex of voltage-dependent anion channel (VDAC) and Hexokinase II (HkII) at the outer mitochondrial membrane. Phosphorylation of VDAC (54) as well as phosphorylation of the transcription factor ATF2, which then attenuates apoptosis through saving the VDAC/Hk interaction (55), are discussed as mechanisms for the prosurvival features of PKC ϵ . The association between the glycolytic enzyme HkII and VDAC has been reported to be specific for cancer cell mitochondria and thus its disruption promises tumor cell specific apoptosis (44). Inhibition of PKC ϵ leads to the MPT due to loss of VDAC/Hk complex as well as loss of inactivated Bad, both of which could be clearly demonstrated for Chondramide treatment. Our work provides evidence for the MPT as target in apoptosis induction by PKC ϵ inhibition in Chondramide treated cells. Data show that Cyclosporine A, which normally blocks the Ca²⁺-induced MPT, is not able to prevent mitochondrial swelling (i.e. the MPT) in isolated mitochondria from cells treated with Chondramide, thus further supporting the involvement of MPT. Moreover, our data offer an explanation how changes in actin cytoskeleton dynamics lead to cell death and proposes the actin cytoskeleton as a specific antitumor target.

4.1.4 Chondramide is a selective indirect inhibitor of PKC ϵ

As mentioned above identification of isozyme selective modulators of PKCs has been a major challenge taken up by various approaches such as the development of ATP-competitive small-molecule inhibitors that bind to the catalytic domain of the kinase, phorbol ester derivatives that mimic the binding of diacylglycerol, or peptides which prevent the anchoring of the PKC to its RACK (receptor of activated C-kinase), which brings the activated enzyme to its substrate (79). Our data propose Chondramide as an indirect PKC ϵ specific inhibitor based on the fact that particularly PKC ϵ due to its actin binding site is trapped by Chondramide induced actin polymerization. The role of PKC ϵ as a promising tumor specific therapeutic target and as a major player in Chondramide induced tumor cell death is supported by two facts: first, non-tumor cells (MCF-10A breast epithelial cells) showing level of PKC ϵ are not sensitive to Chondramide. Second, PKC ϵ overexpression leading to more free PKC ϵ which is not trapped in actin bundles, rescues Chondramide induced apoptosis.

Importantly, Chondramide shows *in vivo* efficacy. Treatment of mice bearing a xenograft breast tumor (MDA-MB-231 cells) with Chondramide leads to reduction of tumor growth by inducing apoptosis through PKC ϵ trapping in actin bundles as shown by immunostainings. Besides this fact, Chondramide treatment is also well tolerable *in vivo* which was monitored by mouse body weight that did not decrease during the treatment period, thus demonstrating the principle feasibility of actin-stabilizers as potential tumor therapeutics.

Our data link actin, a target distributed in all eukaryotic cells to the cancer-specific protein PKC ϵ and open new therapeutical approaches by using actin-overpolymerizing compounds. Thus our work encourages comprehensive pharmacological evaluation of this class of actin-targeting agents in tumor therapy.

4.2 Pharmacological characterization of actin-binding (-)-Doliculide

Another part of this work was to characterize the natural compound doliculide, an actin-overpolymerizing agent, with regard to its cellular effects. The actin binding properties of doliculide were first described by Bai et al. in 2002 (14). The authors showed, that doliculide replaces fluorescent phalloidin from actin filaments and proposed a similar binding site of doliculide to the actin filament. Furthermore, Bai et al. performed a molecular modeling study in which other actin-overpolymerizing compounds like Jasplakinolide, Phalloidin, Chondramide C and Doliculide were mathematically compared. They suggest Doliculide as “core” pharmacophore of these four actin-overpolymerizing compounds (14).

4.2.1 Doliculide inhibits actin dynamics

These previous results primed Doliculide for further pharmacological investigations in our laboratory. To get closer insights in the early influence of Doliculide on the actin CSK we performed FRAP analysis. It was shown that Doliculide leads to a very rapid inhibition of actin dynamics in MCF7 breast cancer cells. First effects were detectable after just eight (!) minutes of incubation, which reflects an extremely good membrane permeability of Doliculide. Actin staining by Rhodamin-Phalloidin of MCF7 and MDA-MB-231 cells reinforced the data obtained by Bai et al., illustrating Doliculide-induced bundling of actin to amorphous clumps.

4.2.2 Doliculide inhibits functional parameters and induces apoptosis

For a closer characterization as potential anti-cancer compound we examined the effects on proliferation and migration, which were also inhibited by Doliculide in low concentrations. It is known, that several other actin-binding compounds participate in the induction of apoptosis, however no closer mechanistic insights are available up-to-date (22, 83). In line with these studies, Doliculide leads to cell death in both cell lines. Activation of Caspase 9 and the cleavage of Poly-(ADP)-ribonucleotid-Polymerase (PARP), common hallmarks of apoptosis, were detectable as well.

Our work defines Doliculide as a potent agent against breast cancer cells lines, which strongly inhibits proliferation and migration and induces apoptosis. Furthermore, these data set the stage for a closer investigation of Doliculide to establish the actin CSK as potential anti-cancer target.

4.3 The potential of actin targeting compounds in cancer therapy

In my work I investigated the cell death inducing mechanism only with Chondramide A. Nonetheless, I claim that the mechanism of trapping PKC ϵ in actin agglomerates is similar between all actin-overpolymerizing compounds and might be a class effect. Dolicolide also leads to the agglomeration of actin in which PKC ϵ might be trapped as well. The formation of actin agglomerates is also known for Jasplakinolide (76). One can argue that the feasibility of *in vivo* trials with Chondramide could be conferrable to other actin-overpolymerizers, too. Moreover, the tolerability in the *in vivo* model encourages for further preclinical investigations concerning pharmacokinetic properties and closer examinations of highly actin depending organs like the muscle of the heart. Next to the cell death induction of actin overpolymerizing compounds described in this work, the actin CSK plays also pivotal roles in other processes concerning cancer malignancies: Magdalena Menhofer could show in her work, that Chondramide inhibits metastasis and angiogenesis (84, 85), thereby increasing the therapeutic potential of actin binders, too.

4.4 Future perspectives

Modern chemotherapies use combinations of anti-cancer drugs to deal with the disease. Thus, potential combination partners for Chondramide should be examined as well. This investigation already started in some respect by combining Chondramide and several other established or experimental chemotherapeutic. Among these compounds are drugs like Doxorubicin, an often used chemotherapeutic in clinic. Another combination based on the fact that PKC ϵ is inhibited by Chondramide is the combination with a STAT3 inhibitor (Stattic) that showed synergistic effects on cell death in combination with Chondramide in preliminary *in vitro* studies (data not shown). Furthermore, drug targeting strategies can also be performed for Chondramide. Conceivable are targeting strategies using Chondramide coupled antibodies directed against cancer cell epitopes or charging nanoparticles with Chondramide to improve the cancer site specific delivery of the compound. Furthermore, the compounds used in this study are not perfect drug molecules concerning their yield during synthesis and their solubility characteristics. Thus, Chondramide and Dolicolide can be used as leads to further improve the structure thereby simplifying the molecule and increasing the solubility in water. Thereby, making this compound class more interesting for the pharmaceutical industry and exploiting the potential of actin-binding compounds in cancer therapy.

5 SUMMARY

Targeting the cytoskeleton (CSK) of cancer cells offers a valuable strategy in cancer therapy. Whereas drugs which address microtubule CSK such as vinca alkaloids or taxanes are well established in the clinic, compounds binding to the actin CSK are still far away from their therapeutical application. One reason might be the lacking knowledge on their mode of cytotoxicity and moreover their tumor specific mechanism of action.

We used the myxobacterial compound Chondramide as a tool to first elucidate the mechanisms of cytotoxicity by actin targeting in different breast cancer cells, namely MCF7 and MDA-MB-231. Chondramide inhibits actin filament assembly and dynamics shown by a fluorescence-based analysis (FRAP) in whole cells and leads to apoptosis characterized by phosphatidylserine exposure, release of cytochrome C from mitochondria and finally activation of caspases (-9 and -3). Detailed analysis revealed, that Chondramide induces apoptosis by enhancing the occurrence of mitochondrial permeability transition (MPT). Known MPT-modulators were found to be affected by Chondramide: Hexokinase II (HkII) bound to the voltage dependent anion channel (VDAC) translocated from the outer mitochondrial membrane to the cytosol and the proapoptotic protein Bad was recruited to the mitochondria. Importantly, PKC ϵ , a prosurvival serine/threonine kinase possessing an actin-binding site and known to regulate the HkII/VDAC interaction as well as Bad phosphorylation was identified as the link between actin CSK and apoptosis induction. PKC ϵ which was found overexpressed in breast cancer cells accumulated in actin bundles induced by Chondramide and lost its activity.

The second goal of our work was to inform on a potential tumor specific action of actin binding agents such as Chondramide. As the nontumor breast epithelial cell line MCF-10A in fact shows resistance to Chondramide induced apoptosis and notably express very low level of PKC ϵ we claim that trapping PKC ϵ via Chondramide induced actin hyperpolymerization displays tumor cell specificity.

Our work provides a link between targeting the ubiquitously occurring actin CSK and selective inhibition of pro-tumorigenic PKC ϵ , thus setting the stage for actin-stabilizing agents as innovative cancer drugs. This is moreover supported by the *in vivo* efficacy of Chondramide triggered by abrogation of PKC ϵ signaling shown in a xenograft breast cancer model.

For the actin targeting compound Dolicolide we could show that Dolicolide impairs the dynamics of the actin CSK similar to Chondramide. Moreover, it reduces the proliferation rate and migration of cancer cells and also leads to the induction of apoptosis, thus Dolicolide is also an interesting lead structure for further preclinical investigations.

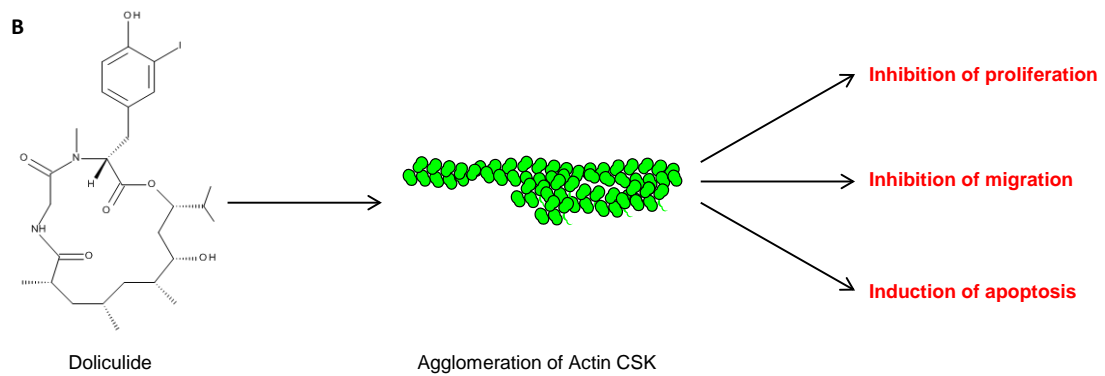
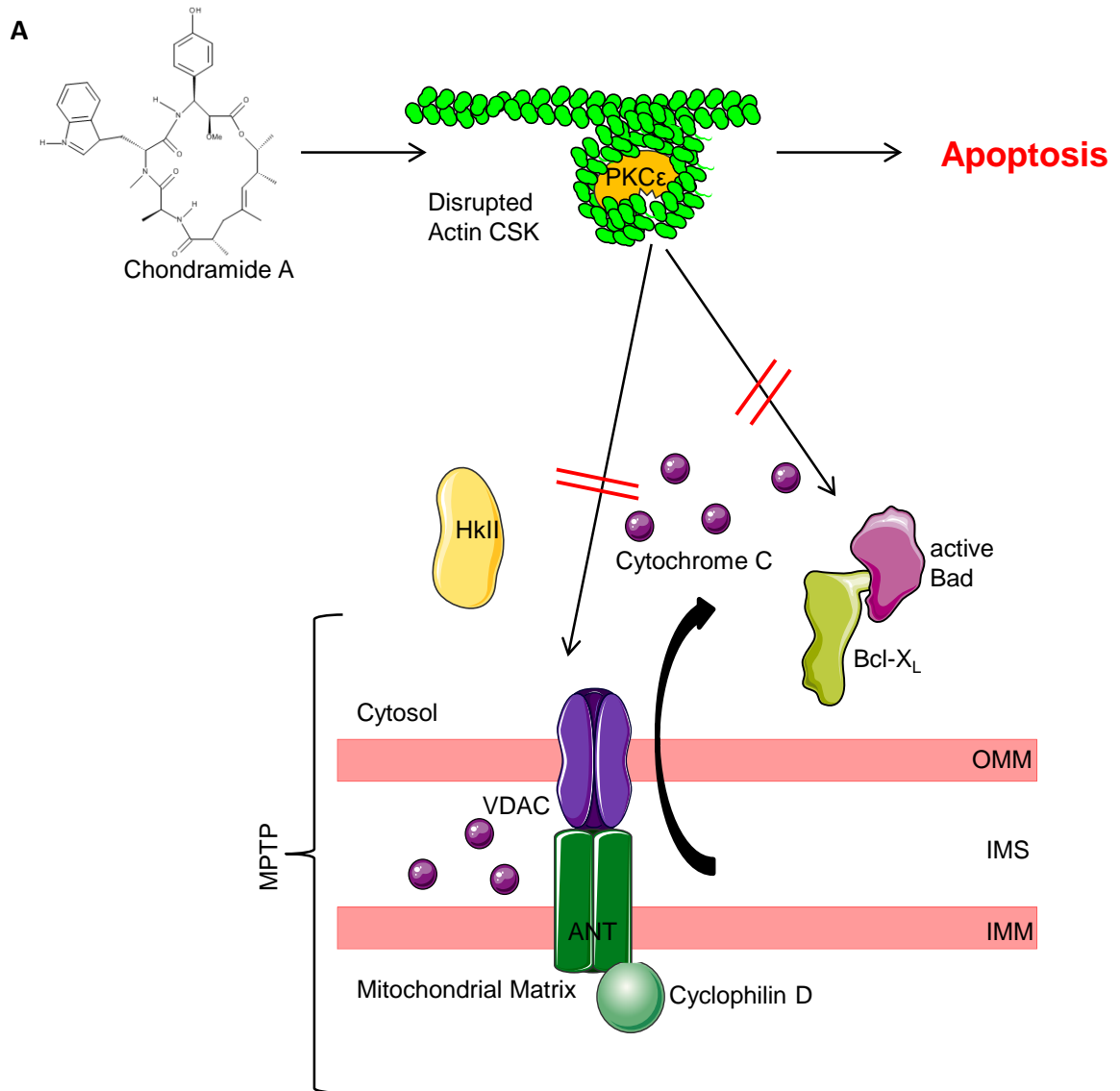


Figure 5.1: (A) Summary of the mechanism of action of Chondramide A. Chondramide A leads to the disruption of the actin cytoskeleton (CSK) by overpolymerizing it and forming agglomerates, containing actin and proteins with an actin-binding site like PKC ϵ . Downstream signaling of PKC ϵ is impaired resulting in opening of the MPTP via the disruption of the interaction between the voltage-dependent anion channel (VDAC) and Hexokinase II (HKII) and the dephosphorylation of Bad, which finally leads to the induction of apoptosis. ANT = Adenosin nucleotide translocase; OMM = outer mitochondrial membrane; IMS = intermembrane space; IMM = inner mitochondrial membrane. (B) Summary of Dolicolide's effects: Dolicolide leads to an agglomeration of actin. Concomitantly, Dolicolide inhibits proliferation, migration and induces apoptosis.

6 REFERENCES

1. Institute NC. Available from: <http://seer.cancer.gov/statfacts/html/breast.html>
2. Singletary SE, Connolly JL. Breast cancer staging: working with the sixth edition of the AJCC Cancer Staging Manual. *CA Cancer J Clin* 2006; **56**: 37-47; quiz 50-31
3. Foulkes WD, Shuen AY. In brief: BRCA1 and BRCA2. *J Pathol* 2013; **230**: 347-349
4. Kreienberg R. Interdisziplinäre S3-Leitlinie für die Diagnostik, Therapie und Nachsorge des Mammakarzinoms. 2012 Available from: http://www.awmf.org/uploads/tx_szleitlinien/032-045OL_k_S3__Brustkrebs_Mammakarzinom_Diagnostik_Therapie_Nachsorge_2012-07.pdf
5. Charehbili A, Fontein DB, Kroep JR, Liefers GJ, Mieog JS, Nortier JW, et al. Neoadjuvant hormonal therapy for endocrine sensitive breast cancer: a systematic review. *Cancer Treat Rev* 2014; **40**: 86-92
6. Jelovac D, Emens LA. HER2-directed therapy for metastatic breast cancer. *Oncology (Williston Park)* 2013; **27**: 166-175
7. Tacar O, Sriamornsak P, Dass CR. Doxorubicin: an update on anticancer molecular action, toxicity and novel drug delivery systems. *J Pharm Pharmacol* 2013; **65**: 157-170
8. Gornstein E, Schwarz TL. The paradox of paclitaxel neurotoxicity: Mechanisms and unanswered questions. *Neuropharmacology* 2014; **76 Pt A**: 175-183
9. Holohan C, Van Schaeybroeck S, Longley DB, Johnston PG. Cancer drug resistance: an evolving paradigm. *Nat Rev Cancer* 2013; **13**: 714-726
10. Weissman KJ, Muller R. Myxobacterial secondary metabolites: bioactivities and modes-of-action. *Nat Prod Rep* 2010; **27**: 1276-1295
11. von Schwarzenberg K, Vollmar AM. Targeting apoptosis pathways by natural compounds in cancer: marine compounds as lead structures and chemical tools for cancer therapy. *Cancer Lett* 2013; **332**: 295-303
12. Kunze B, Jansen R, Sasse F, Hofle G, Reichenbach H. Chondramides A approximately D, new antifungal and cytostatic depsipeptides from *Chondromyces crocatus* (myxobacteria). Production, physico-chemical and biological properties. *J Antibiot (Tokyo)* 1995; **48**: 1262-1266
13. Ghosh AK, Liu C. Total synthesis of antitumor depsipeptide (-)-doliculide. *Org Lett* 2001; **3**: 635-638
14. Bai R, Covell DG, Liu C, Ghosh AK, Hamel E. (-)-Doliculide, a new macrocyclic depsipeptide enhancer of actin assembly. *J Biol Chem* 2002; **277**: 32165-32171
15. Schmauder A, Sibley LD, Maier ME. Total synthesis and configurational assignment of chondramide A. *Chemistry* 2010; **16**: 4328-4336
16. Allingham JS, Klenchin VA, Rayment I. Actin-targeting natural products: structures, properties and mechanisms of action. *Cell Mol Life Sci* 2006; **63**: 2119-2134
17. Lorenz M, Popp D, Holmes KC. Refinement of the F-actin model against X-ray fiber diffraction data by the use of a directed mutation algorithm. *J Mol Biol* 1993; **234**: 826-836
18. Oda T, Namba K, Maeda Y. Position and orientation of phalloidin in F-actin determined by X-ray fiber diffraction analysis. *Biophys J* 2005; **88**: 2727-2736
19. Steinmetz MO, Stoffler D, Muller SA, Jahn W, Wolpensinger B, Goldie KN, et al. Evaluating atomic models of F-actin with an undecagold-tagged phalloidin derivative. *J Mol Biol* 1998; **276**: 1-6
20. Bubb MR, Senderowicz AM, Sausville EA, Duncan KL, Korn ED. Jasplakinolide, a cytotoxic natural product, induces actin polymerization and competitively inhibits the binding of phalloidin to F-actin. *J Biol Chem* 1994; **269**: 14869-14871
21. Schweikart K, Guo L, Shuler Z, Abrams R, Chiao ET, Kolaja KL, et al. The effects of jaspamide on human cardiomyocyte function and cardiac ion channel activity. *Toxicol In Vitro* 2013; **27**: 745-751

22. Franklin-Tong VE, Gourlay CW. A role for actin in regulating apoptosis/programmed cell death: evidence spanning yeast, plants and animals. *Biochem J* 2008; **413**: 389-404
23. Pollard TD, Cooper JA. Actin, a central player in cell shape and movement. *Science* 2009; **326**: 1208-1212
24. Perrin BJ, Ervasti JM. The actin gene family: function follows isoform. *Cytoskeleton (Hoboken)* 2010; **67**: 630-634
25. Bugyi B, Carlier MF. Control of actin filament treadmilling in cell motility. *Annu Rev Biophys* 2010; **39**: 449-470
26. Pollard TD. Regulation of actin filament assembly by Arp2/3 complex and formins. *Annu Rev Biophys Biomol Struct* 2007; **36**: 451-477
27. Burute M, Thery M. Spatial segregation between cell-cell and cell-matrix adhesions. *Curr Opin Cell Biol* 2012; **24**: 628-636
28. Kerr JF, Wyllie AH, Currie AR. Apoptosis: a basic biological phenomenon with wide-ranging implications in tissue kinetics. *Br J Cancer* 1972; **26**: 239-257
29. Kroemer G, Galluzzi L, Brenner C. Mitochondrial membrane permeabilization in cell death. *Physiol Rev* 2007; **87**: 99-163
30. Hanahan D, Weinberg RA. Hallmarks of cancer: the next generation. *Cell* 2011; **144**: 646-674
31. Wyllie AH, Kerr JF, Currie AR. Cell death: the significance of apoptosis. *Int Rev Cytol* 1980; **68**: 251-306
32. Taylor RC, Cullen SP, Martin SJ. Apoptosis: controlled demolition at the cellular level. *Nat Rev Mol Cell Biol* 2008; **9**: 231-241
33. Fiandalo MV, Kyprianou N. Caspase control: protagonists of cancer cell apoptosis. *Exp Oncol* 2012; **34**: 165-175
34. Kantari C, Walczak H. Caspase-8 and bid: caught in the act between death receptors and mitochondria. *Biochim Biophys Acta* 2011; **1813**: 558-563
35. Fogg VC, Lanning NJ, Mackeigan JP. Mitochondria in cancer: at the crossroads of life and death. *Chin J Cancer* 2011; **30**: 526-539
36. Green DR, Kroemer G. The pathophysiology of mitochondrial cell death. *Science* 2004; **305**: 626-629
37. Leibowitz B, Yu J. Mitochondrial signaling in cell death via the Bcl-2 family. *Cancer Biol Ther* 2010; **9**: 417-422
38. Brenner C, Grimm S. The permeability transition pore complex in cancer cell death. *Oncogene* 2006; **25**: 4744-4756
39. Galluzzi L, Kepp O, Trojel-Hansen C, Kroemer G. Mitochondrial control of cellular life, stress, and death. *Circ Res* 2012; **111**: 1198-1207
40. Galluzzi L, Kepp O, Kroemer G. Mitochondria: master regulators of danger signalling. *Nat Rev Mol Cell Biol* 2012; **13**: 780-788
41. Elrod JW, Molkentin JD. Physiologic functions of cyclophilin D and the mitochondrial permeability transition pore. *Circ J* 2013; **77**: 1111-1122
42. McGee AM, Baines CP. Phosphate is not an absolute requirement for the inhibitory effects of cyclosporin A or cyclophilin D deletion on mitochondrial permeability transition. *Biochem J* 2012; **443**: 185-191
43. Schmitt S, Saathoff F, Meissner L, Schropp EM, Lichtmannegger J, Schulz S, et al. A semi-automated method for isolating functionally intact mitochondria from cultured cells and tissue biopsies. *Anal Biochem* 2013:
44. Galluzzi L, Kepp O, Tajeddine N, Kroemer G. Disruption of the hexokinase-VDAC complex for tumor therapy. *Oncogene* 2008; **27**: 4633-4635
45. Roy SS, Madesh M, Davies E, Antonsson B, Danial N, Hajnoczky G. Bad targets the permeability transition pore independent of Bax or Bak to switch between Ca²⁺-dependent cell survival and death. *Mol Cell* 2009; **33**: 377-388
46. Newton AC. Regulation of the ABC kinases by phosphorylation: protein kinase C as a paradigm. *Biochem J* 2003; **370**: 361-371

47. Steinberg SF. Structural basis of protein kinase C isoform function. *Physiol Rev* 2008; **88**: 1341-1378
48. Akita Y. Protein kinase C-epsilon (PKC-epsilon): its unique structure and function. *J Biochem* 2002; **132**: 847-852
49. Prekeris R, Hernandez RM, Mayhew MW, White MK, Terrian DM. Molecular analysis of the interactions between protein kinase C-epsilon and filamentous actin. *J Biol Chem* 1998; **273**: 26790-26798
50. Basu A, Sivaprasad U. Protein kinase Cepsilon makes the life and death decision. *Cell Signal* 2007; **19**: 1633-1642
51. Aziz MH, Manoharan HT, Church DR, Dreckschmidt NE, Zhong W, Oberley TD, et al. Protein kinase Cepsilon interacts with signal transducers and activators of transcription 3 (Stat3), phosphorylates Stat3Ser727, and regulates its constitutive activation in prostate cancer. *Cancer Res* 2007; **67**: 8828-8838
52. Garg R, Blando J, Perez CJ, Wang H, Benavides FJ, Kazanietz MG. Activation of nuclear factor kappaB (NF-kappaB) in prostate cancer is mediated by protein kinase C epsilon (PKCepsilon). *J Biol Chem* 2012; **287**: 37570-37582
53. Suzuki A, Goto Y, Iguchi T. Progression of PDMT is accompanied by lack of Fas and intense expression of Bcl-2 and PKC-epsilon. *Carcinogenesis* 1997; **18**: 883-887
54. Baines CP, Song CX, Zheng YT, Wang GW, Zhang J, Wang OL, et al. Protein kinase Cepsilon interacts with and inhibits the permeability transition pore in cardiac mitochondria. *Circ Res* 2003; **92**: 873-880
55. Lau E, Kluger H, Varsano T, Lee K, Scheffler I, Rimm DL, et al. PKCepsilon promotes oncogenic functions of ATF2 in the nucleus while blocking its apoptotic function at mitochondria. *Cell* 2012; **148**: 543-555
56. Meshki J, Caino MC, von Burstin VA, Griner E, Kazanietz MG. Regulation of prostate cancer cell survival by protein kinase Cepsilon involves bad phosphorylation and modulation of the TNFalpha/JNK pathway. *J Biol Chem* 2010; **285**: 26033-26040
57. Mischak H, Goodnight JA, Kolch W, Martiny-Baron G, Schaechtle C, Kazanietz MG, et al. Overexpression of protein kinase C-delta and -epsilon in NIH 3T3 cells induces opposite effects on growth, morphology, anchorage dependence, and tumorigenicity. *J Biol Chem* 1993; **268**: 6090-6096
58. Caino MC, Lopez-Haber C, Kissil JL, Kazanietz MG. Non-small cell lung carcinoma cell motility, rac activation and metastatic dissemination are mediated by protein kinase C epsilon. *PLoS One* 2012; **7**: e31714
59. Song MS, Park YK, Lee JH, Park K. Induction of glucose-regulated protein 78 by chronic hypoxia in human gastric tumor cells through a protein kinase C-epsilon/ERK/AP-1 signaling cascade. *Cancer Res* 2001; **61**: 8322-8330
60. Pan Q, Bao LW, Kleer CG, Sabel MS, Griffith KA, Teknos TN, et al. Protein kinase C epsilon is a predictive biomarker of aggressive breast cancer and a validated target for RNA interference anticancer therapy. *Cancer Res* 2005; **65**: 8366-8371
61. Okhrimenko H, Lu W, Xiang C, Hamburger N, Kazimirsky G, Brodie C. Protein kinase C-epsilon regulates the apoptosis and survival of glioma cells. *Cancer Res* 2005; **65**: 7301-7309
62. Toton E, Ignatowicz E, Skrzeczkowska K, Rybczynska M. Protein kinase Cepsilon as a cancer marker and target for anticancer therapy. *Pharmacol Rep* 2011; **63**: 19-29
63. Cenni V, Doppler H, Sonnenburg ED, Maraldi N, Newton AC, Toker A. Regulation of novel protein kinase C epsilon by phosphorylation. *Biochem J* 2002; **363**: 537-545
64. Murakoshi H, Lee SJ, Yasuda R. Highly sensitive and quantitative FRET-FLIM imaging in single dendritic spines using improved non-radiative YFP. *Brain Cell Biol* 2008; **36**: 31-42

65. Sasse F, Kunze B, Gronewold TM, Reichenbach H. The chondramides: cytostatic agents from myxobacteria acting on the actin cytoskeleton. *J Natl Cancer Inst* 1998; **90**: 1559-1563
66. Crowder RN, El-Deiry WS. Caspase-8 regulation of TRAIL-mediated cell death. *Exp Oncol* 2012; **34**: 160-164
67. Reubold TF, Eschenburg S. A molecular view on signal transduction by the apoptosome. *Cell Signal* 2012; **24**: 1420-1425
68. Pastorino JG, Hoek JB. Regulation of hexokinase binding to VDAC. *J Bioenerg Biomembr* 2008; **40**: 171-182
69. Matcha K, Madduri AV, Roy S, Ziegler S, Waldmann H, Hirsch AK, et al. Total synthesis of (-)-doliculide, structure-activity relationship studies and its binding to F-actin. *Chembiochem* 2012; **13**: 2537-2548
70. Hall A. The cytoskeleton and cancer. *Cancer Metastasis Rev* 2009; **28**: 5-14
71. Mollinedo F, Gajate C. Microtubules, microtubule-interfering agents and apoptosis. *Apoptosis* 2003; **8**: 413-450
72. Dumontet C, Jordan MA. Microtubule-binding agents: a dynamic field of cancer therapeutics. *Nat Rev Drug Discov* 2010; **9**: 790-803
73. Wertz IE, Kusam S, Lam C, Okamoto T, Sandoval W, Anderson DJ, et al. Sensitivity to antitubulin chemotherapeutics is regulated by MCL1 and FBW7. *Nature* 2011; **471**: 110-114
74. Furst R, Vollmar AM. A new perspective on old drugs: non-mitotic actions of tubulin-binding drugs play a major role in cancer treatment. *Pharmazie* 2013; **68**: 478-483
75. Posey SC, Martelli MP, Azuma T, Kwiatkowski DJ, Bierer BE. Failure of gelsolin overexpression to regulate lymphocyte apoptosis. *Blood* 2000; **95**: 3483-3488
76. Bubb MR, Spector I, Beyer BB, Fosen KM. Effects of jasplakinolide on the kinetics of actin polymerization. An explanation for certain in vivo observations. *J Biol Chem* 2000; **275**: 5163-5170
77. Lazaro-Dieguez F, Aguado C, Mato E, Sanchez-Ruiz Y, Esteban I, Alberch J, et al. Dynamics of an F-actin aggresome generated by the actin-stabilizing toxin jasplakinolide. *J Cell Sci* 2008; **121**: 1415-1425
78. Zeidman R, Troller U, Raghunath A, Pahlman S, Larsson C. Protein kinase Cepsilon actin-binding site is important for neurite outgrowth during neuronal differentiation. *Mol Biol Cell* 2002; **13**: 12-24
79. Mochly-Rosen D, Das K, Grimes KV. Protein kinase C, an elusive therapeutic target? *Nat Rev Drug Discov* 2012; **11**: 937-957
80. Oliva JL, Caino MC, Senderowicz AM, Kazanietz MG. S-Phase-specific activation of PKC alpha induces senescence in non-small cell lung cancer cells. *J Biol Chem* 2008; **283**: 5466-5476
81. Newton PM, Messing RO. The substrates and binding partners of protein kinase Cepsilon. *Biochem J* 2010; **427**: 189-196
82. Chiang CW, Kanies C, Kim KW, Fang WB, Parkhurst C, Xie M, et al. Protein phosphatase 2A dephosphorylation of phosphoserine 112 plays the gatekeeper role for BAD-mediated apoptosis. *Mol Cell Biol* 2003; **23**: 6350-6362
83. Celeste Morley S, Sun GP, Bierer BE. Inhibition of actin polymerization enhances commitment to and execution of apoptosis induced by withdrawal of trophic support. *J Cell Biochem* 2003; **88**: 1066-1076
84. M. H. Menhofer DB, R. Kubisch, J. Busse, E. Wagner, R. Müller, A. M. Vollmar, S. Zahler. In vitro and in vivo characterization of the actin polymerizing compound Chondramide as angiogenic inhibitor. *submitted* 2014:
85. M. H. Menhofer RK, L. Schreiner, M. Zorn, F. Förster, R. Mueller, J. O. Rädler, E. Wagner AMV, S. Zahler. The actin targeting compound Chondramide inhibits breast cancer metastasis via reduction of cellular contractility. 2014:

7 Appendix

7.1 Publications

7.1.1 Original publications

Förster F., Braig S., Moser C., Kubisch R., Busse J., Wagner E., Schmoeckel E., Mayr D., Schmitt S., Huettel S., Müller R. and Vollmar A.M. Targeting the actin cytoskeleton: selective anti-tumor action via trapping PKC ϵ . *Cell Death & Disease*. submitted

Förster F., Braig S., Chen T., Altmann KH. And Vollmar A.M. Pharmacological characterization of actin-binding (-)-Doliculide. *Bioorganic & Medicinal Chemistry*. Accepted March 6, 2014

7.1.2 Poster presentations

Förster F., von Schwarzenberg K., Müller R., Vollmar A.M. *Chondramide A inhibits cancer cell growth by the induction of apoptosis and senescence.*

Natural Anti-cancer Drugs, June 30 – July 4, 2012, Olomouc, Czech Republic

Förster F., von Schwarzenberg K., Müller R., Vollmar A.M. *The actin cytoskeleton as potential antitumor target: Chondramide and its effects on breast cancer cells.*

DPhG Annual Meeting 2012, October 10-13, Greifswald, Germany

Förster F., Braig S., Vollmar A.M. *Myxobacterial Chondramide A: distinct apoptotic action at mitochondria is mediated via targeting the actin cytoskeleton.*

25. Irseer Naturstofftage, February 20-22, Irsee, Germany

Förster F., Braig S., Zischka H., Müller R., Vollmar A.M. *Linking the actin cytoskeleton to the mitochondrial apoptosis pathway by myxobacterial compound Chondramide A.*

1st European Conference on Natural Products: Research and Applications, September 22-25, 2013, Frankfurt, Germany

Förster F., Braig S., Zischka H., Müller R., Vollmar A.M. *Pharmacological disruption of the actin cytoskeleton contributes to the induction of intrinsic apoptosis.* The 21st ECDO

Euroconference on Apoptosis; Cell death, a Biomedical Paradigm; September 25-28, 2013, Paris, France

7.1.3 Oral presentations

Förster F., von Schwarzenberg K., Vollmar A.M. *Chondramide and Pretubulysin inhibit breast cancer cell proliferation*. 2nd FOR 1406 meeting, October 26, 2011, München, Germany

Förster F., Braig S., Vollmar A.M. *Chondramide induces apoptosis via the mitochondrial cell death pathway*. 3rd FOR 1406 Meeting, September 16-18, 2012, Feldafing, Germany

Förster F., Braig S., Vollmar A.M. *Chondramide A and its way to induce cancer cell death*. 4th FOR 1406 Meeting, July 16-18, 2013, Saarbrücken, Germany

7.1.4 Awards

“ECDO Best Poster Award” for: *Pharmacological disruption of the actin cytoskeleton contributes to the induction of intrinsic apoptosis* on the 21st ECDO Euroconference on Apoptosis; Cell death, a Biomedical Paradigm; September 25-28, 2013, Paris, France

7.2 Acknowledgements

Mein herzlichster Dank geht an Frau Prof. Dr. Angelika Vollmar für die Möglichkeit in den letzten drei Jahren wissenschaftliches Arbeiten zu erlernen und zu vertiefen, um diese Arbeit anfertigen zu können. Ebenso möchte ich mich für die Möglichkeit bedanken viele Konferenzen besucht haben zu können und Teil der FOR 1406 gewesen zu sein, was eine sehr interessante und bereichernde Erfahrung gewesen ist. Vielen Dank auch für die wertvollen Diskussionen persönlicher und wissenschaftlicher Art und die warme und herzliche Art, die im Arbeitskreis Grundlage für eine sehr gute und ausgewogene Stimmung ist. Darüber hinaus vielen Dank für die Freiheit eigene Ideen und Konzepte zu entwickeln, zu falsifizieren oder eben auch zu verifizieren.

Ein weiteres Dankeschön gilt Herrn Prof. Dr. Stefan Zahler für die Unterstützung bei mikroskopischen, wie auch anderen Fragestellungen und der Bereitschaft als Zweitgutachter für die Dissertation zur Verfügung zu stehen.

Ebenfalls möchte ich recht herzlich den anderen Teilnehmern der Prüfungskommission danken, namentlich Herrn Prof. Dr. Wagner, Herrn Prof. Dr. Frieß, Herrn Prof. Dr. Paintner und Herrn PD. Dr. Michalakis.

Im Rahmen dieser Arbeit hatte ich auch die Gelegenheit mit vielen Kooperationspartnern zusammen zu arbeiten und Einblicke in andere Arbeitsweisen zu erhalten. Hierbei gilt mein Dank Dr. Rebekka Kubisch, Johanna Busse und Prof. Dr. Ernst Wagner für die Durchführung der Tierversuche, Dr. Schmoeckel und Dr. Mayr für die Bereitstellung von Brustgewebe und Sabine Schmitt und Dr. Hans Zischka bei der Durchführung der Mitochondrienversuche.

Ein weiteres Dankeschön möchte ich an Karin von Schwarzenberg richten, die mir im ersten Teil meiner Promotion mit Rat und Tat zu Seite stand.

Ein herzlicher Dank gilt auch Christina Moser, die im Rahmen dieser Arbeit ihre Masterarbeit angefertigt hat, und sehr zum Erfolg dieses Projekts beigetragen hat.

Liebe Simone, dir möchte ich für die Unterstützung und Geduld danken, die du die ganze Zeit aufgebracht hast. Besonders für die vielen Zigarettenpausen mit wissenschaftlichen und privaten Themen und die ein oder andere, im wahrsten Sinne des Wortes, zündende Idee.

Liebe Magdalena, vielen Dank für so manches Gespräch und die Bereitschaft Menschen neu ein zu schätzen.

Liebe Tini, dir meinem Labor-Companion vielen Dank für die wissenschaftlichen, lustigen und ernsten Momente in den letzten drei Jahren. Schön jemanden wie dich kennengelernt zu haben.

Ich möchte auch dem gesamten Arbeitskreis für das freundschaftliche und produktive Klima danken, das hier in den letzten drei Jahren vorgeherrscht hat. Es ist mir auch weiterhin jeden Tag eine Freude unsere Flure zu betreten und so nette Kollegen vor zu finden.

Besonders danken möchte ich den Doktoranden aus meiner Generation Michi, Verena, Lena, Tini und Sandra. Wir haben gemeinsam so einiges erlebt und die sommerlichen Grillabende bleiben unvergesslich.

Zu guter Letzt möchte ich meinen Eltern Marianne und Walter (†19.07.2012) für alles danken, was sie mir ermöglicht haben. Der Rückhalt und Zusammenhalt auch in schweren Zeiten war unvergleichlich.